

MDPI

Review

# MOF-Based Catalysts for Thermal Hydrogenation of CO<sub>2</sub> to HCOOH: A Review

Zechen Ye 10, Wenxuan Xie 20 and Hongyan Chen 3,\*0

- Department of Chemical and Biomolecular Engineering, National University of Singapore, Singapore 117576, Singapore; e0022634@u.nus.edu
- <sup>2</sup> Waste Water Treatment Plant, Yuancheng District, Heyuan 517099, China
- School of Chemistry and Materials Engineering, Huizhou University, Huizhou 516007, China
- \* Correspondence: chenhy@hzu.edu.cn

## **Abstract**

The  $CO_2$  emission issue has raised global concern as the sea level increase it caused can threaten human activity. The utilization of  $CO_2$  as a building block for value-added chemicals can be an effective approach for the mitigation of the greenhouse effect. As one of the potential valuable products, formic acid (HCOOH) has been recognized as an effective hydrogen carrier. For thermal  $CO_2$ -to-HCOOH conversion, molecular catalysts and metal nanoparticles are prominent choices for the initial conversion. The conventional catalyst substrates have been shown to have issues of deactivation and product selectivity. The metal–organic framework (MOF), as a novel catalyst substrate, showcases its potential for solving the problem. Herein, this review intends to provide an overview of recent progress of metal nanoparticles and molecular catalysts stabilized by conventional catalyst substrates and MOFs for thermal  $CO_2$ -to-HCOOH conversion, including perspectives on further research.

**Keywords:** metal–organic frameworks; molecular catalysts; metal nanoparticles; CO<sub>2</sub> hydrogenation; formic acid; encapsulation; synergy effects



Academic Editor: Jorge Bedia and Iian Oi

Received: 7 September 2025 Revised: 5 October 2025 Accepted: 11 October 2025 Published: 14 October 2025

Citation: Ye, Z.; Xie, W.; Chen, H. MOF-Based Catalysts for Thermal Hydrogenation of CO<sub>2</sub> to HCOOH: A Review. *Catalysts* **2025**, *15*, 978. https://doi.org/10.3390/catal15100978

Copyright: © 2025 by the authors. Licensee MDPI, Basel, Switzerland. This article is an open access article distributed under the terms and conditions of the Creative Commons Attribution (CC BY) license (https://creativecommons.org/licenses/by/4.0/).

# 1. Introduction

High energy demand due to boosted economic growth has led to heavy consumption of fossil fuels, resulting in massive emissions of carbon dioxide (CO<sub>2</sub>) in the air [1]. A promising solution to reduce carbon emissions is to convert CO<sub>2</sub> into formic acid (HCOOH), an essential chemical used in the leather and textile industries for tanning and dyeing [2]. Against this background, high-performance catalysts for such CO<sub>2</sub> conversion have been targeted.

Since the discovery of triphenylphosphine-based Ru, Rh, and Ir complexes by Inoue et al. [3], there has been tremendous progress in the field of homogenous catalysis towards formic acid (HCOOH) synthesis by direct CO<sub>2</sub> conversion. Generally, three main factors, namely catalyst, solvent, and reaction conditions, can affect the harvest of HCOOH [4]. To develop an efficient homogeneous catalyst, scientists have devoted extensive efforts to screen a variety of transition metals (e.g., Pd, Ni, Fe, Cu, Ru, Rh, and Ir) and organic ligands (e.g., phosphorous ligands, C,N- and N,N-chelated ligands, N-heterocyclic carbine ligands, and pincer ligands) [5]. For example, Ru/Ir-pincer complexes were found to possess outstanding activities for CO<sub>2</sub> reduction, offering an impressive turnover number (TON) and turnover frequency (TOF) up to 3,500,000 and 1,100,000 h<sup>-1</sup>, respectively [6]. In

terms of solvent effect, the chemical nature (i.e., polarity, pH value, and ability to donate proton) plays a decisive role. Specifically, highly polar solvents with strong hydrogen bonds can improve HCOOH yield through the solvation of reactants and products. For instance, polar solvents (i.e., MeOH, water, and DBU) can boost HCOOH yield [7–10], while aprotic solvents (i.e., THF, MeCN, DMSO, and DMF) perform poorly [11]. In addition, CO<sub>2</sub> in supercritical condition was demonstrated to yield an effective hydrogenation reaction [8,12], highlighting the critical role served by reaction condition.

To date, homogeneous catalysts have been well recognized for their excellent performance in promoting HCOOH productivity. Nonetheless, the capacity to convert CO<sub>2</sub> per unit time and reactor volume is far from ideal due to the ultralow catalyst concentration used [13]. For real applications, the additional cost for catalyst separation, reusability, and stability is another challenge and therefore makes them economically unfeasible for HCOOH production on a domestic scale [14]. On the other hand, heterogeneous catalysts, with their desirable production rate from an industrial perspective as well as easy handling and excellent reusability, have been identified as promising candidates to address the challenges associated with homogeneous catalysts, generating increasing interest in exploring heterogenous catalysts in this field [6]. For this, metal complexes (MCs) and metal nanoparticles (MNPs) offer significant advantages. One shows high selectivity under mild conditions and tunability for specific pathways [15,16], and the other presents high catalytic activities with abundant under-coordinated active sites. The catalyst substrates for the stabilization of these catalysts are commonly organic nano-supports, inorganic oxides, or metal oxides [4,17–20]. Nonetheless, they suffer from metal aggregation and poor tunability on selective CO<sub>2</sub> hydrogenation [21]. This limitation, however, can be overcome by metal-organic frameworks (MOFs), which have also been recognized as highly porous coordination materials. This concept of MOFs has been well established since Yaghi's seminal research in 1995 [22]. This breakthrough catalyzed exponential growth in their influence across materials chemistry and engineering disciplines. A pivotal advancement emerged in 1999 when the same research team synthesized the archetypal [Zn<sub>4</sub>O(BDC)<sub>3</sub>] architecture (BDC = 1,4-benzenedicarboxylate), labelled as MOF-5 [23]. It has become one of the most extensively characterized MOF benchmarks, lying as a cornerstone for further studies of MOFs with various chemical and physical properties [24] (e.g., molecular-sieving effect by pre-selected pore matrix; the inhibition of agglomeration of MNP; and higher catalytic performance than individual counterparts by synergizing with guest molecules) [25]. With this in mind, MOF-confined MCs or MNPs have shown promising potential on thermal CO<sub>2</sub> hydrogenation [26,27]. Herein, this review aims to introduce the development progress of conventional heterogeneous catalysts and MOF-based catalysts for CO<sub>2</sub> conversion, as well as future research directions.

# 2. Conventional Heterogeneous Catalysts

## 2.1. Noble Catalysts

Historically, the first work on heterogeneous catalysts for HCOOH synthesis dates back to the Pd-catalyzed reduction of KHCO<sub>3</sub> by Bredig and Carter in 1914 [28]. However, poor activity and the rapid deactivation of metal particles became a problem due to rapid aggregation and poor dispersion. Despite decades of pioneering works on this theme, such issues were not effectively solved until the application of heterogeneous supports [29].

Generally, the Pd catalyst is attractive due to its excellent capacity to absorb and dissociate H<sub>2</sub> molecules, but presents poor performance for CO<sub>2</sub> activation [30]. Nitrogen-doped carbon substrates are complementary to Pd catalysts because their abundant N-containing functional groups can serve as basic sites for CO<sub>2</sub> activation [4]. As demonstrated by Chang Won Yoon et al. [31] in 2014, HCOOH could be obtained from a CO<sub>2</sub>/H<sub>2</sub> mixture

Catalysts **2025**, 15, 978 3 of 20

using a Pd/mpg-C<sub>3</sub>N<sub>4</sub> catalyst, for which N-functionalities in mpg-C<sub>3</sub>N<sub>4</sub> were suggested to serve for multiple purposes. As determined by rich electron densities, they not only present an efficient abstraction of CO<sub>2</sub> but also suppress the aggregation of Pd nanoparticles (NPs), thus facilitating HCOOH production [32]. Similarly, Lee et al. [33] exploited Pd/g-C<sub>3</sub>N<sub>4</sub> catalysts for HCOOH synthesis without the aid of a base and demonstrated that  $0.6 \text{Pd/g-C}_3 \text{N}_4$  afforded the highest PTY (Pd total yield), up to 413.5  $\mu$ mol mol<sub>Pd</sub><sup>-1</sup>s<sup>-1</sup>, while PTY plunge was observed over the Pd catalyst loaded on nitrogen-free carbon nanotubes. In addition, a monotonic relationship was established between Pd particle size and catalytic activity, with a two-fold increase in TOF over Pd/C<sub>3</sub>N<sub>4</sub> while Pd particle size was decreased from 7.2 to 3.4 nm. The characterization of small-sized Pd catalysts showed a growing number of interfacial sites between Pd NPs and g-C<sub>3</sub>N<sub>4</sub>, which were banked on the HCOOH formation. On this basis, a hypothetical mechanism was proposed: CO<sub>2</sub> and H<sub>2</sub> were initially activated by g-C<sub>3</sub>N<sub>4</sub> and Pd particles, respectively, followed by a migration towards interfacial sites for HCOOH formation. Following these successes, edge defects have been further explored, as demonstrated by Perez-Ramirez et al. [34], who improved catalytic behavior by maximizing the number of defective edge sites on g-C<sub>3</sub>N<sub>4</sub> substrate, achieving 20 times TOF of HCOOH with respect to the best Pd/g-C<sub>3</sub>N<sub>4</sub> reported. This study vividly presented a compromise between Pd loading and metal agglomeration, intending for the optimal delivery of H atoms as requested by CO<sub>2</sub> reduction.

For a long time, metal oxides, unlike carbon-based substrates, received little interest due to their inferior activity, and this gridlock was resolved by Yan's group [35]. Specifically, CO<sub>2</sub> reduction into HCOOH over Pd/ZnO and Pd/CeO<sub>2</sub> was investigated to understand the reaction process, during which diffuse reflectance infrared Fourier transform spectroscopy (DRIFTS) was used to monitor reaction intermediates over the catalyst surface. With DRIFTS, the bicarbonate formation was captured as the key species for formate (HCOO) synthesis. As a result of rivalry between Pd/ZnO and Pd/CeO<sub>2</sub>, the former possessed negligible basic properties; however, the abundant basic sites of Pd/CeO<sub>2</sub> rendered it a different story, turning the governing step from bicarbonate formation to H<sub>2</sub> dissociation instead. Stemming from such fundamental understanding, two crucial features were identified towards the rational design of advanced catalysts, namely sufficient basic sites to promote CO<sub>2</sub> activation and small Pd particles responsible for H<sub>2</sub> splitting. Driven by the aforementioned principles, more efficient Pd catalysts were developed using TiO<sub>2</sub> to carry more basic sites than either ZnO or CeO<sub>2</sub> to disperse Pd particles, eventually offering a large TOF of 909 h<sup>-1</sup> for HCOOH production, substantially higher than Pd/CeO<sub>2</sub> and Pd/ZnO.

Other than the Pd catalyst, Ru also shows its appealing catalytic nature by its superior production of HCOOH. As to Ru-complex immobilization, silica is one of the preferred substrates due to its high specific surface area for catalyst impregnation and irreducible and inert properties [36]. Zheng et al. [37] extended an amine functionalized silica with immobilized Ru complexes coupled with ethanol for HCOOH synthesis. The  $\rm CO_2$  hydrogenation was conducted at 16 MPa and 80 °C in the presence of PPh3 for 1 h, yielding 100% selectivity of HCOOH with 1384 h<sup>-1</sup> TOF. Aside from  $\rm SiO_2$ ,  $\rm Al_2O_3$ , characterized by high specific surface area and appreciable stability, is another eligible choice. Zhao's group [38] achieved a yield for FA of up to 731 h<sup>-1</sup> TOF using a Y-Al2O3 nanorod supported Ru catalyst in the presence of ethanol and NEt3 as a solvent and an additive, respectively. As noted above, the support seems crucial to Ru catalytic activity as the blossom of hydroxyl groups on its surface can not only offer strong metal-support interactions with Ru components but also facilitate  $\rm CO_2$  adsorption, thus enhancing Ru reactivity [39]. However, other factors including gas partial pressure, solvents, and ligands can also have significant impacts upon HCOOH productivity and should not be overlooked [40]. For example, a

Catalysts **2025**, 15, 978 4 of 20

supercritical condition could improve the dissolvability of H<sub>2</sub> and boost CO<sub>2</sub> diffusion, therefore promoting the productivity of HCOOH. Zheng et al. [41] found that TOF was doubled by jumping from  $600 \text{ h}^{-1}$  to  $1197 \text{ h}^{-1}$  on the [Si-(CH<sub>2</sub>)<sub>3</sub>-NH<sub>2</sub>-Ru] catalyst when CO<sub>2</sub> was in supercritical condition. Given the unique properties of ionic liquids, such as negligible vapor pressure, wide liquid temperature range, and high thermal stability, they have been widely considered as excellent solvents to extract HCOOH and accelerate reaction rate. Han et al. [42] initially introduced an ionic liquid [mammim][TfO] to promote CO<sub>2</sub> hydrogenation catalyzed by a silica-immobilized Ru complex. However, the production rate was not adequate, as indicated by low TOF(103 h<sup>-1</sup>), which was significantly improved to 920 h<sup>-1</sup> with a new ionic liquid [DAMI][TFO] towards Ru-catalyzed CO<sub>2</sub> hydrogenation [43]. Srivastava [44] conducted a comparison study between Ru/MCM-41 and Ru/SiO<sub>2</sub>, and the former was found to be superior. In addition, a series of functionalized ionic liquids were prepared and screened for Ru/MCM-41-catalyzed CO<sub>2</sub> reduction, identifying [DAMI][CF<sub>3</sub>CF<sub>2</sub>CF<sub>2</sub>SO<sub>3</sub>] as the best with the maximum TON value of 17,787 and without significant deactivation of the Ru/MCM-41 catalyst after a 10-cycle run. It has been demonstrated that ligands can privilege reactivity by forming active species with catalyst precursors. Wang et al. [45] synthesized Ru-DBU/Al<sub>2</sub>O<sub>3</sub> catalysts for CO<sub>2</sub> hydrogenation and demonstrated HCOOH production with a TOF of 239 h<sup>-1</sup>, which could be notably improved to 751  $h^{-1}$  by replacing ligand DBU with PPh<sub>3</sub> [46].

Apart from Ru and Pd, other metals have also been active on HCOOH synthesis. For example, Hicks et al. [47] reported CO<sub>2</sub> reduction using mesoporous silica-tethered iridium complex, Ir-PN/SBA-15, presenting a maximum yield of  $1.2 \times 10^{-3} \text{ h}^{-1}$  at 120 °C, 4.0 MPa, and 2 h; moreover, this catalyst showed high durability as evidenced by the slight decrement for TON after 10 cycles. Later, they developed a new catalyst (PEI-PN/Ir) by coordinating an Ir precursor with iminophospine-tethered polyethyleneimine (PEI) to optimize CO<sub>2</sub> capture and conversion [48]. It was revealed that transforming 65% of available primary amines on PEI into PN/Ir active sites could yield an optimal balance between CO<sub>2</sub> capture and conversion, attaining the highest production rate of HCOOH. Fachinetti et al. [49] reported stable activity for the heterogeneous Au catalyst (Au/TiO<sub>2</sub>) with an amine solvent, demonstrating high selectivity (83% for HCOOH) and excellent durability highlighted by only minor performance change even after a 37-day run. In 2016, Hensen et al. [50] proposed an investigation on CO<sub>2</sub> hydrogenation performance over a number of supported and unsupported Au catalysts, with Au/Al<sub>2</sub>O<sub>3</sub> identified as the best performer, which outperformed Au/TiO<sub>2</sub> by doubling the productivity. These studies highlight the crucial role of support in determining the catalytic activity of MNP catalysts.

### 2.2. Bimetallic Catalysts

The unique catalytic behavior of bimetallic NPs has demonstrated merit in heterogeneous catalysis, as demonstrated by various combinations. Taking the Fe-Ru catalyst as an example, it greatly increased HCOOH production with a TON of 318 in contrast to relatively poor performance obtained from monometallic Ru NPs [51]. Pd, as the first constituent widely used for CO<sub>2</sub>-to-HCOOH synthesis, has been extensively modified with various transition metals (i.e., Ag, Au, Co, and Mn) [29] to mediate its electronic and geometric properties, leading to optimized catalytic performance.

In 2018, Yamashita et al. [52] synthesized a PdAg/TiO<sub>2</sub> catalyst to promote CO<sub>2</sub> hydrogenation. The PdAg alloy composition was studied by varying the Ag concentration while keeping Pd loading at 1.0 wt%. A curve with a volcano shape was observed in the relationship between catalytic activity and Pd/Ag ratio. Neither Pd/TiO<sub>2</sub> nor Ag/TiO<sub>2</sub> could achieve an effective catalysis, demonstrating the pivotal role of synergism between Pd and Ag. The composition's impact was investigated by preparing a series of catalysts

Catalysts **2025**, 15, 978 5 of 20

(i.e., Pd/TiO<sub>2</sub>, Ag@Pd/TiO<sub>2</sub>, PdAg/TiO<sub>2</sub>, and Pd@Ag/TiO<sub>2</sub>), and Pd@Ag/TiO<sub>2</sub> was discovered to be the best. Its exceptional catalytic activity was explained by the rich electronic state of Pd particles, donated by surrounding Ag neighbors. Density functional theory (DFT) calculations further revealed that the electrons gained by Pd particles facilitated more negative hydride species, resulting in decrease of activation barrier for bicarbonate hydrogenation, which was the rate determining step. To further improve catalytic activity, this group introduced amine moieties to the support [53], specifically using phenylaminefunctionalized SBA-15 to immobilize PdAg NPs. The weak basicity of phenylamine could transform the catalytic nature of PdAg NPs by tuning not only their particle size but also their CO<sub>2</sub> adsorption property, thus achieving a TON of 874 for HCOOH; however, the underlying mechanism remains unclear. A follow-up study was therefore performed using a phenylamine-functionalized-mesoporous-carbon-supported PdAg alloy [54], in which the activation barrier for reduction of phenylamine-facilitated bicarbonate was 32.1 kcal/mol. The N-containing functional group was found to be the principal component that formed H-bonds with bicarbonate for its stabilization. In addition, they discovered a proportional relationship between the catalytic activity and nitrogen content of phenylamine [55]. Given that the PdAg alloy has higher amine levels, it led to a surge of adsorption energy of bicarbonate accompanied by a plummet in the activation barrier of its hydrogenation, indicative of catalytic promotion by phenylamine. Thus, amine functionalization benefits the reaction via four mechanisms: (i) CO<sub>2</sub> capture; (ii) smaller-nanoparticle formation; (iii) bicarbonate reduction; and (iv) electron donation to Pd.

Non-noble metals, privileging cost-effective catalysis, appear as an attractive option to alloy with Pd NPs. For instance, Nguyen and co-workers [56] proposed an efficient Pd-Ni/CNT-GR catalyst for base-free CO<sub>2</sub> hydrogenation into HCOOH, achieving a two-fold increase in TOF with respect to Pd/CNT-GR. The rationale behind this was the synergistic interaction with Ni, which enriched the electron densities of the Pd side due to charge transfer, under which electron-rich Pd could benefit  $H_2$  dissociation with Ni at an electron-deficient state profitable for CO<sub>2</sub> activation, thus leading to higher catalytic activity.

## 2.3. Cu-Based Catalysts

Despite a plethora of activity related to Cu catalysts in methanol synthesis, there have been fewer inroads on HCOOH synthesis. The ground-breaking publication came from Bada et al. [57], who reported the first attempt for catalyzing HCOOH synthesis by an effective homogeneous catalyst, Cu(OAc)<sub>2</sub>·H<sub>2</sub>O-1,2-bis(diphenylphosphino)-benzene, achieving TOF =  $1350 \text{ h}^{-1}$  of HCOOH. There have been a number of consecutive works demonstrating the high reactivity of homogeneous Cu catalysts, but they are impractical for industrial-scale production due to low reusability, highlighting the strong demand for high stability [58]. Lin et al. [59] impregnated commercial Cu catalysts (Cu/ZnO/Al<sub>2</sub>O<sub>3</sub> in Cu:Zn:Al = 5:2:3 molar ratio) at various calcination temperatures, and the one prepared at 300 °C showed the best catalytic behavior, delivering 13.11% CO<sub>2</sub> conversion and 7.82% yield of HCOOH with 59.62% selectivity. In addition, they studied various reaction temperatures for direct CO<sub>2</sub> conversion into HCOOH using Cu/CuCr<sub>2</sub>O<sub>4</sub>, from which a proportional relationship of Cu activity and operating temperature was derived below 140 °C but followed by an activity crash upon further increases in temperature [60]. The highest CO<sub>2</sub> conversion (14.6%) was achieved when the reaction temperature was modulated at 140 °C, showing a HCOOH yield of 12.8% with 87.8% selectivity.

## 2.4. Metal Oxides

Beyond Cu-based catalysts, Fe-, Mn-, and Al-based oxides are competitive catalysts due to their low cost and natural abundance [61]. Jin and co-workers [62–64] evaluated

Catalysts 2025, 15, 978 6 of 20

MnO, as obtained via the dehydration of Mn(OH)<sub>2</sub> for hydrothermal CO<sub>2</sub> reduction to HCOOH using NaHCO<sub>3</sub> as a promotor for hydrogen production. As a result, more than 75% HCOOH yield was obtained with 98% selectivity. They subsequently examined Al powder, where NaHCO<sub>3</sub> assists Al oxidation in hot water, while only 64% HCOOH was yielded despite impressive improvement in its selectivity (i.e., 100%). Under similar conditions, Fe<sub>3</sub>O<sub>4</sub> displayed markedly higher productivity than MnO and Al<sub>2</sub>O<sub>3</sub>, as presented in Table 1.

**Table 1.** Conventional heterogenous catalysts for hydrogenation of CO<sub>2</sub> to HCOO/HCOOH, where T and P are denoted to be temperature and pressure, respectively. NA means "not reported".

Catalyst	T/°C	Solvent	P <sub>CO2</sub> /P <sub>H2</sub> (MPa/MPa)	TON	Ref.
Ru-PPh <sub>3</sub> /Al <sub>2</sub> O	80	H <sub>2</sub> O/EtOH/NEt <sub>3</sub>	2.0/2.0	751	[46]
Ir-PN/SBA-15	60	NEt <sub>3</sub> aq.	6.0/6.0	2800	[47]
PEI-PN/Ir	120	NEt <sub>3</sub> aq.	20.0/20.0	1240	[48]
"Si"-(CH <sub>2</sub> ) <sub>3</sub> NH(CSCH <sub>3</sub> )- {RuCl <sub>3</sub> (PPh <sub>3</sub> )}	60	[DAMI][TfO]	9.0/9.0	109	[43]
Ru/MCM-41	80	NEt <sub>3</sub> aq.	20.0/20.0	2019	[44]
(Si)-NH <sub>2</sub> -RuCl <sub>3</sub>	80	scCO <sub>2</sub> /EtOH/NEt <sub>3</sub>	12.0/4.0	1481.5	[41]
Ru-DBU/Al <sub>2</sub> O <sub>3</sub>	80	DMSO/NEt <sub>3</sub> /KH <sub>2</sub> PO <sub>4</sub> /EtOH	6.0/9.0	239	[45]
Ru/γ-Al <sub>2</sub> O <sub>3</sub>	80	EtOH/NEt <sub>3</sub>	1.35/0.5	12.5	[38]
Pd/CeO <sub>2</sub>	40	1 M NaOH/KOH/NEt <sub>3</sub> aq.	7/7	909	[35]
Ru/SiO <sub>2</sub> - (CH <sub>2</sub> ) <sub>3</sub> NH(CH <sub>2</sub> ) <sub>3</sub> CH <sub>3</sub>	80	EtOH	12/4	1384	[37]
Pd/ECN-1h	40	H <sub>2</sub> O	2.5/2.5	1520	[34]
Pd/g-C <sub>3</sub> N <sub>4</sub>	40	H <sub>2</sub> O	25/25	17.7	[33]
Si-(CH <sub>2</sub> ) <sub>3</sub> NH(CSCH <sub>3</sub> )-RuCl <sub>3</sub> - PPh <sub>3</sub>	60	EtOH/[mammim][TfO]	5.5/5.5	500	[42]
Au/Al <sub>2</sub> O <sub>3</sub>	70	EtOH/NEt <sub>3</sub>	4.0/4.0	215	[50]
Au/TiO <sub>2</sub>	40	NEt <sub>3</sub>	2.1/2.1	18,040	[49]
PdAg/TiO <sub>2</sub>	100	1M NaHCO <sub>3</sub> aq.	1.0/1.0	748	[52]
PdAg/SBA-15-phenylamine	100	1M NaHCO <sub>3</sub> aq.	1.0/1.0	874	[53]
PdAg/amine-MSC	100	1M NaHCO₃ aq.	1.0/1.0	839	[54]
PdAg/amine-RF10	100	1M NaHCO <sub>3</sub> aq.	1.0/1.0	867	[55]
Pd <sub>3</sub> Ni <sub>7</sub> /CNT-GR	40	H <sub>2</sub> O	2.5/2.5	5.4	[56]
Cu(OAc) <sub>2</sub> ·H <sub>2</sub> O-1,2- bis(diphenylphosphino)- benzene	100	1,4-dioxane	0.1/NA	8100	[57]
Cu/ZnO/Al <sub>2</sub> O <sub>3</sub>	140	$H_2O$	3.0/3.0	6.17	[59]
Cu/CuCr <sub>2</sub> O <sub>4</sub>	140	1M NaHCO₃ aq.	1.5/1.5	4.19	[60]
MnO	300	1M NaHCO₃ aq.	NA	0.06	[62]
$Al_2O_3$	300	1M NaHCO₃ aq.	NA	0.11	[63]
Fe <sub>3</sub> O <sub>4</sub>	300	2M NaHCO <sub>3</sub> aq.	NA/6.0	38	[64]

Catalysts **2025**, 15, 978 7 of 20

# 3. MOF-Based Catalysts

MOF design integrates three essential elements: molecular building blocks, predefined topological nets, and isoreticular chemistry [65]. Building blocks comprise inorganic secondary building units (SBUs) and multitopic organic linkers, which serve as the molecular components for framework assembly [66]. Topological nets provide the architectural blueprint for MOF construction, representing spatial connectivity patterns through vertexand-edge notation [67]. These nets constitute the primary design phase, establishing the underlying structural topology prior to chemical functionalization (Figure 1). Isoreticular chemistry enables the precise modulation of material properties while preserving the target topology [68]. This approach facilitates the strategic selection and combination of building blocks to tune chemical functionality, porosity, and stability parameters critical for optimizing performance in different fields. Thanks to isoreticular chemistry, MOFs are highly versatile in a wide range of applications as introduced in many reviews [24,69–72]. For example, the tunable pores, by modulation of organic linkers, enable the capture of selective-size adsorbates [73]; the exchange of SBU enhances MOF stability in different chemical environments [74]; and the incorporation of external metal dopant into the SBU node of the MOF for the amelioration of catalytic activity by bimetallic synergy [75].

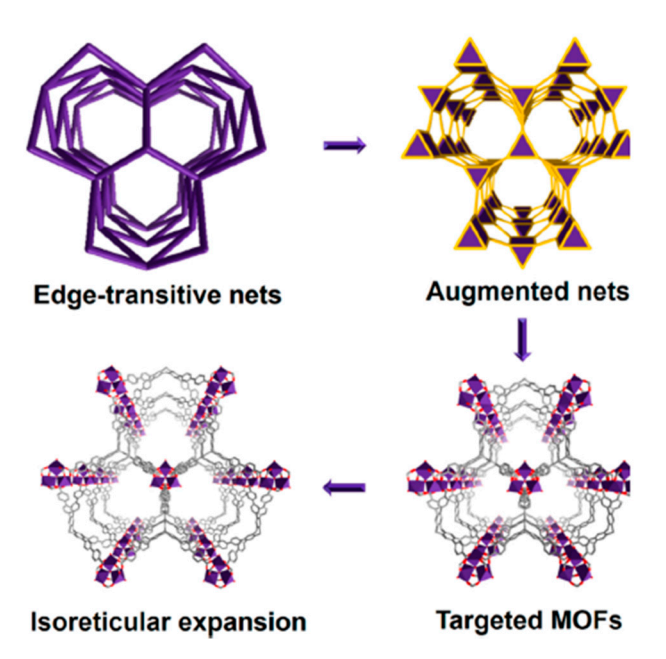


**Figure 1.** Illustration of MOF design, synthesis, and isoreticular expansion based on edge-transitive nets [67]. Adapted from ref. [67], with permission from American Chemistry Society, copyright 2022.

## 3.1. MOF-Supported and MOF-Derived Catalysts

Early MOF-supported hydrogenation catalysts include Pd/MOF-5 for styrene and cis-cyclooctene, introduced by Kaskel et al. [76] in 2007. Soon after, the first surface-anchored molecular catalyst was reported by Kholdeeva et al., reporting the experimental synthesis of metal-polyoxometalate (M-POM) on MIL-101 for α-pinene allylic oxidation and caryophyllene epoxidation with hydrogen peroxide [77]. Since then, it has spurred a worldwide impetus for the development of MOF-supported catalysts. Still, there is a severe lack of literature reporting the use of MOFs for the thermal hydrogenation of CO<sub>2</sub> to HCOOH thus far [78–80]. Instead, scientists pursue the photoreduction or electroreduction of CO<sub>2</sub> to HCOOH, with a focus on green chemistry and higher product selectivity [81–83]. In 2019, Wang et al. [84] examined a series of azolium-MOF supported Ru complexes (i.e., RuCl<sub>3</sub>, [RuCp\*Cl<sub>2</sub>]<sub>2</sub>, and [Ru(C<sub>6</sub>Me<sub>6</sub>)Cl<sub>2</sub>]<sub>2</sub>, where Cp\* and C<sub>6</sub>Me<sub>6</sub> are pentamethylcyclopentadienyl and hexamethylbenzene, respectively) for CO<sub>2</sub> hydrogenation to

Catalysts **2025**, 15, 978 8 of 20

HCOOH.  $[Ru(C_6Me_6)Cl_2]_2/MOF$  shows the highest performance by delivering TON = 3803 at 120 °C and 8 Mpa, attributed to the stronger electron-donating capacity of the C<sub>6</sub>Me<sub>6</sub> ligand, which is conducive to CO<sub>2</sub> hydrogenation. Ji et al. [85] anchored the PdAg alloy on various amine functionalized MIL-101 and found PdAg/TEDA-MIL-101-NH2 brought the highest activity with TON = 1500 at 70 °C after 10 h. In 2020, Mehlana et al. [86] doped Pd (II) in Mg:JMS-2a and Mn:JMS-2a for CO<sub>2</sub> hydrogenation to HCOO in basic solutions. The experimental results revealed higher productivity and stability on the latter, with TON = 9809 after 24 h. In 2023, this group used a similar approach to introduce noble metal complexes (i.e., an Ir(III) pentamethylcyclopentadienyl dimer, Rh(III) pentamethylcyclopentadienyl dimer, (p-cymene)Ru(II) chloride dimer, bis-(acetonitrile)Pd dichloride, and Pt tetrachloroplatinate(II)) on JMS-5a for the same reaction [87], among which the Ir(III) and Rh(III) series exhibited the highest activity with TON = 5473 and 4319, respectively. In the same year, Maihom et al. [88] used computational methods to investigate MH-DUT-5 (M = Mn, Fe, Co, Ni, and Cu) MOFs for the hydrogenation of CO<sub>2</sub> to HCOOH, where MH represents metal hydride. They found that NiH-DUT-5 showed the highest activity by offering the lowest activation barrier (=21.5 kcal mol<sup>-1</sup>) for the rate-determining step in the reaction. As demonstrated above, a superb outcome was showcased by the catalysts while using an MOF as a support.

Alternatively, thermal treatment can be applied on an MOF, which serves as a sacrificial template, to produce its derivatives including porous carbon-supported MNPs and metal sulfides, etc., leading to a series of MOF-derived catalysts [70]. Owing to the inherent properties of the parent MOF, such derived catalysts show appreciable catalytic performance for CO<sub>2</sub> hydrogenation, particularly for the formation of methanol [89]. As to HCOOH synthesis, Bordoloi et al. [90] used a combined DFT/experimental method to investigate it over M-CuZn@CNx (M = Ru, Pd, Pt, and Ir), which were derived by the pyrolysis of M-CuZn MOFs. According to DFT calculations, a stepwise mechanism was identified, and the formate (HCOO) pathway was more favorable than the carboxyl (COOH) route over all catalysts. Among these catalysts, Ru–CuZn@CNx exhibited the highest productivity of HCOOH with TON = 11,435 and presented the lowest activation barrier for HCOO formation.

# 3.2. MOF-Confined Catalysts

#### 3.2.1. Synthesis Strategies

The synthesis of MOF-confined catalysts can be branched into four categories, including "ship-in-bottle", "bottle-around-ship", "sandwich assembly strategy", and "in situ encapsulation", as shown in Figure 2 [91]. As many reviews have provided a full description of synthesis methods [92-97], we herein briefly introduce the strategies in this section. The "shipin-bottle" strategy entails the introduction of a metal-ligand complex into the channels of a pre-formed MOF with or without a subsequent reduction process to form the composite [98]. The reducing agent is required for the synthesis of MNP@MOF with an aim of reducing the metal precursor into an MNP after infiltrating it into the MOF matrix (Figure 2(a-1)) [99], but is not required for the encapsulation of the MC in the MOF [100]. For the bottle-around-ship strategy, a pre-synthesized MC or MNP is introduced into the MOF precursor solution with commitment growth of the MOF framework around it (Figure 2b) [101]. There is another method of synthesis for the MNP@MOF, where the encapsulation of the metal precursor through ligand design is performed prior to the assembly of the MOF, with consecutive reduction using a chemical agent (Figure 2(a-2)) [91]. Similarly, the synthesis of the MC@MOF using this method requires no chemical agent. Figure 2c refers to sandwich assembly, typically serving for the synthesis of the MNP@MOF [93]. It initiates with a separately synthesized MOF and MNP and then deposits the MNP onto the MOF through a stabilizing solvent. If the catalyst is sufficiently small to penetrate into the MOF, it will distribute on both the internal and external surface of the MOF. Alternatively, it will be deposited on the external surface of

the MOF. Finally, an outer MOF shell is epitaxially overgrown around the MOF@catalyst. The in situ encapsulation is a time and cost-effective strategy (Figure 2d) [79], which involves the mixing of precursors of both the MOF and catalyst in a single reactor. As a result, the MOF and catalyst are produced simultaneously and assembled into a single nanostructure with balanced experimental parameters.

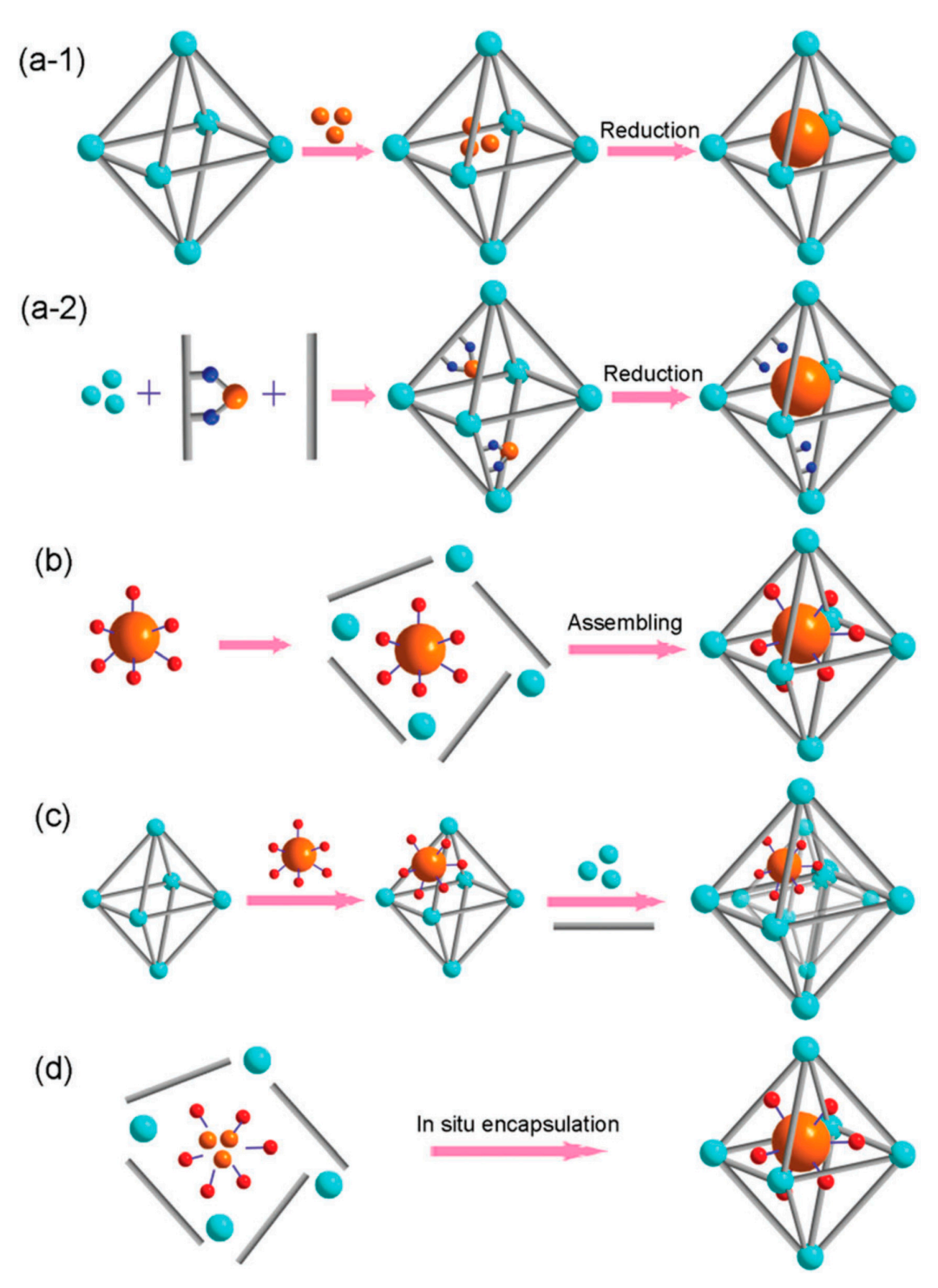


**Figure 2.** Fabrication strategies for MC or MNP encapsulation in MOFs: (a) ship-in-bottle, including (a-1) post-assembly incorporation of NE precursors and (a-2) pre-assembly incorporation of metal precursors, (b) bottle-around-ship, (c) sandwich assembly, and (d) in situ encapsulation. Cyan, SBUs of MOFs; gray, organic linkers; orange, metal precursor; and red, stabilizing agents [91]. Adapted from ref. [91] with permission from The Royal Society of Chemistry, copyright 2014.

## 3.2.2. Catalysis

The potential of MOF-confined catalysts was first demonstrated by Fischer's group with Pd NPs loaded in MOF-5 [102]. The unique synergistic functions as well as combined properties of NPs and MOFs led to notably high activity for CO oxidation, where electron donation and confinement contributed to such improvement. Generally,  $CO_2$  has been viewed as an electron acceptor rather than an electron donor [103]; therefore, electron-rich environments and basic sites within MOF pores can effectively modulate active sites' electronics and stabilize intermediates involved in  $CO_2$  hydrogenation, as demonstrated below.

In 2019, Zhao's group [104] synthesized a series of RuCl<sub>3</sub>-anchored MIL-101-Cr catalysts for CO<sub>2</sub> hydrogenation, including RuCl<sub>3</sub>@MIL-101-Cr-NH<sub>2</sub>, RuCl<sub>3</sub>@MIL-101-Cr-Sal, and RuCl<sub>3</sub>@MIL-101-Cr-DPPB. Sal (salicylaldehyde) and DPPB were used as linker agents to functionalize MIL-101-Cr-NH<sub>2</sub>, in which Schiff-base moieties were produced by condensation with amino group. RuCl<sub>3</sub>@MIL-101-Cr-DPPB was recognized as the best candidate, delivering the most productive yield of formic acid with TON = 242 (120  $^{\circ}$ C and 6 MPa). For such superior performance, the first and foremost reason was that the amino group and Schiff-base moieties could act as electron donors for the Ru metal center, making it more active towards CO<sub>2</sub> activation and hydrogenation. Another reason was stronger coordination interaction between RuCl<sub>3</sub> and DPPB. With the complement of an assortment of polar solvents (DMSO, water, and 3 mmol PPh<sub>3</sub>), it could result in an almost quadruple growth of TON value, being up to 831. This was interpreted as the combination of the extraordinarily high polarity of DMSO, and improved miscibility between Et<sub>3</sub>N and DMSO by water and electron donation to the Ru center by PPh3 ligands. In this work, DPPB was found to enhance catalytic activity by donating electrons to the Ru center, but the effect was not pronounced due to the weak electron-donating nature of the amino group. Additionally, the electron-donating effect was not deeply studied using a theoretical analysis tool.

To address the above issues, the same group selected ZIF-8-Mtz (Mtz = 3-methyl-1,2,4-triazole), introducing abundant N-laced moieties as electron donors for RuCl $_3$  immobilization [105]. With such a strategy, TON = 372 was achieved for HCOOH synthesis, from the contribution of imidazole C and N to electron delivery towards the empty orbital of Ru and their synergistic interaction increasing the electron density around Ru. As revealed by DFT calculations, an energy barrier of 8.81 kcal/mol for CO $_2$  activation was obtained. The imidazole C from the organic linker could also act as an electron donor because of the conjugated electronic structure of the imidazole ring, providing an electron bath around the ring that both C and N could soak in. Hence, RuCl $_3$ @ZIF-8-Mtz showed better CO $_2$  hydrogenation performance, as evidenced by a TON improved by 100 for HCOOH formation compared to RuCl $_3$ @MIL-101-Cr-DPPB at the same reaction conditions. Moreover, TON can be further increased by nearly triple the amount upon adding a cofeed of water and ethanol. This is because ethanol is a protic solvent and can afford a hydrogen-bonding interaction with CO $_2$ , thus facilitating the nucleophilic attack of Ru-H to CO $_2$  and making the formation of -O-CHO easier [106].

Another similar system was reported by Yamashita et al. [107] who developed a sandwich-like core-shell catalyst ZIF-8@Pd $_1$ Ag $_2$ @ZIF-8 for CO $_2$  reduction to HCOOH. The catalyst was decomposed at 350 °C, demonstrating its relatively high thermostability. In this study, both Ag and basic N groups within ZIF-8 nanopores acted as electron amplifiers for the Pd catalyst. The production rate of HCOOH was notably higher over electron-rich Pd sites in contrast to those in relatively electron-deficient states (e.g., ZIF-8@Pd $_3$ @ZIF-8, Pd $_1$ Ag $_2$ ). In particular, zero activity occurring upon unsupported Pd $_1$ Ag $_2$  was attributed to the agglomeration of nanoparticles. By contrast, ZIF-8 serving as a shell could suppress inter-particle aggregation and enhance activity by highly dispersing Pd $_1$ Ag $_2$  nanoparticles

in its cages. Additionally, MIL-101 was also demonstrated as a promising shell to confine the PdAg alloy. Li's group [108] synthesized PdAg@MIL-101-PEI for HCOO production via the hydrogenation of  $CO_2$ . In this, the catalyst showed stable performance over multiple catalytic cycles as manifested by its structural integrity, as well as a considerable yield of HCOO (i.e., 4968 TON) at 120  $^{\circ}$ C under 8 MPa.

Due to its high hydrothermal and mechanical stability, UiO-66 has been added to a target list for research. In 2017, Lin et al. [109] used it for Ir-complex encapsulation for hydrogenating  $CO_2$  to HCOO/HCOOH in a Soxhlet-type reflux-condensing system, under which a 410 h $^{-1}$ -TOF yield rate of product was obtained under ambient pressure and at 85 °C. A concerted proton-hydride transfer mechanism was proposed by the authors for  $CO_2$  hydrogenation to HCOOH on an Ir complex. In 2018, Tsung et al. [110] achieved aperture-opening encapsulation of the Ru complex by dissociative linker exchange reactions in UiO-66. The authors reported an outstanding productivity of HCOO on Rucomplex@UiO-66, where the yield rate reached approximately 300,000 TON as an average over 5 cycles.

As demonstrated, MOF-confined catalysts have advantages over conventional catalysts in maintaining the integrity of the catalyst (e.g., the high durability of PdAg@MIL-101-PEI) [108], offering multi-functionality due to tailorable chemistry (e.g., MIL-101-NH<sub>2</sub> shows high performance on CO<sub>2</sub> capture and acts as an electron donor to promote its hydrogenation) [85], and synergistic host–guest interactions enhancing catalytic activity (e.g., electron donation by ZIF-8 can enhance the electron density of Ru, thus lowering the energy barrier for CO<sub>2</sub> activation) [105]. With this in mind, it is not surprising that [Ru]@UiO-66 outperformed other catalysts due to its superb productivity (Tables 1 and 2). Nevertheless, this field is currently limited by the following challenges: (i) most MOFs collapse at high temperature except UiO-66 [111]; (ii) high porosity but small-size pores can limit the diffusion of reactants and products, thus resulting in less-than-5000-TON production for most MOF-confined catalysts (Table 2); (iii) the confinement can suppress MNP agglomeration but also reduce the accessibility of the active site to reactants; and (iv) the difficult and time-consuming synthesis of the composite.

**Table 2.** MOF-based catalysts for CO<sub>2</sub> hydrogenation to HCOO/HCOOH, where T and P are denoted to be temperature and pressure, respectively.

Catalyst	T/°C	Solvent	P <sub>CO2</sub> /P <sub>H2</sub> (MPa/MPa)	TON	Ref.
PdAg/TEDA-MIL-101-NH <sub>2</sub>	70	1M NaHCO <sub>3</sub> aq.	2.5/2.5	1500	[85]
Pd@Mg:JMS-2a	100	EtOH	1.25/3.75	7272	[86]
Pd@Mn:JMS-2a	100	EtOH	1.25/3.75	9808	[86]
Ir(III)@JMS-5a	110	EtOH	1.25/3.75	5473	[87]
Rh(III)@JMS-5a	110	EtOH	1.25/3.75	4319	[87]
Ru3-NHC-MOF	120	DMF	4.0/4.0	3803	[84]
Ru-CZ	120	Base-free aq.	4.0/4.0	11,434	[90]
RuCl <sub>3</sub> @MIL-101(Cr)-DPPB	120	DMSO/H <sub>2</sub> O/NEt <sub>3</sub>	3.0/3.0	831	[104]
$RuCl_3@ZIF-8-Mtz(0.29)$	120	EtOH/NEt <sub>3</sub>	4.0/4.0	1416	[105]
ZIF-8@Pd <sub>1</sub> Ag <sub>2</sub> @ZIF-8	100	$1 \text{ M NaHCO}_3 \text{ aq}$ .	1.0/1.0	112	[107]
PdAg@MIL-101-PEI	120	Ethanol/NEt <sub>3</sub>	4.0/4.0	4968	[108]
mbpyOH-[Ir <sup>III</sup> ]-UiO	85	1 M NaHCO₃ aq.	0.1/0.1	6149	[109]
[Ru]@UiO-66	129	DMF/DUB	0.29/3.45	300,000	[110]

## 3.3. Reaction Mechanism

So far, four pathways have presently been recognized for thermal  $CO_2$ -to-HCOOH conversion, including the HCOO pathway, the carboxyl COOH pathway, direct reaction between  $CO_2$  and  $H_2$ , and the concerted pathway [112]. The former two are stepwise path-

ways that, after the dissociative adsorption of the hydrogen molecule, initial hydrogenation of CO<sub>2</sub> occurs to form COOH or HCOO as reaction intermediates and one of which is consecutively converted into HCOOH through a second hydrogenation (Figure 3A,B). The latter two are one-step hydrogenation pathways in which HCOOH is simply formed by attacking C and O atoms of adsorbed CO<sub>2</sub> by two H atoms simultaneously (Figure 3C,D). The only difference between these two pathways is whether catalytic hydrogen dissociation is presented or not.

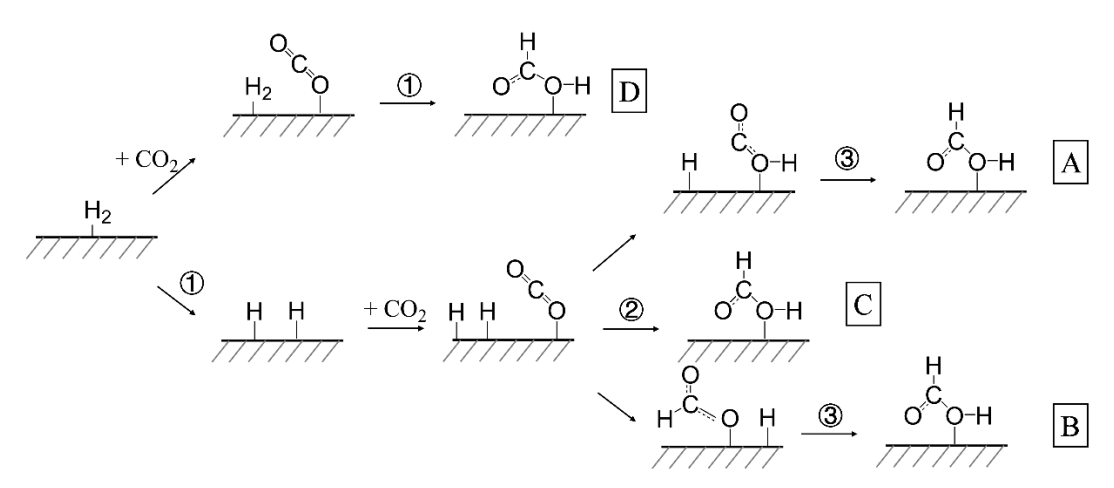


**Figure 3.** Schematic diagram of **(A)** COOH pathway; **(B)** HCOO pathway; **(C)** concerted pathway; and **(D)** direct CO<sub>2</sub> hydrogenation.

In the literature, the mechanistic investigation of thermal CO<sub>2</sub>-to-HCOOH conversion has been extensively studied, with metal node or organic linkers as the active site [113]. The former might or might not require the removal of metal-ligand bonds for the release of its activity [114]. For poorly coordinated MOF, open metal sites are readily available to the reactants. Renaud et al. [115] used MIL-53(Cr) as a CO<sub>2</sub> capturer to assist its conversion on a cyclopentadienyl iron tricarbonyl complex through H-bonding with CO2, which is first hydrogenated into HCOO and then HCOOH. Long et al. [116] reported the reversible binding of CO<sub>2</sub> with subsequent hydrogenation to HCOO on terminal zinc hydride sites of ZnH-MFU-4l. It implies that HCOO is probably a reaction intermediate in HCOOH formation. When it comes to high-connectivity MOFs (e.g., UiO-66), defective engineering is necessary in releasing the active metal sites. Jiang et al. [117] performed a mechanistic study on defective UiO-66 using DFT methods. As shown in Figure 4, one organic linker was removed to free an open space for the adsorption of H<sub>2</sub> and CO<sub>2</sub> on the OH-Zr-O active site—frustrated Lewis pair (FLP). Three pathways were examined (Figure 3B–D) and the concerted pathway was demonstrated to be the most effective route to HCOOH formation, followed by the HCOO pathway. Direct CO<sub>2</sub> hydrogenation presents the lowest kinetics with a notably high energy barrier due to the additional energy required for hydrogen dissociation.

Different from metal nodes, the organic linker is either doped with an external metal atom to form a single-atom catalyst or grafted with functional groups (e.g., -NH<sub>2</sub>) to become active to the adsorbents [118]. For instance, Limtrakul et al. [119] functionalized MOF-5 with Cu alkoxide for the HCOO-pathway-based hydrogenation of CO<sub>2</sub> to HCOOH, where the activation barriers of initial and second hydrogenation are 24.2 and 18.3 kcal mol<sup>-1</sup>, respectively. Mojgan Heshmat [120] fabricated an FLP on UiO-66, where nitrogen acts as a Lewis base and boron as a Lewis acid, to study the concerted hydrogenation of CO<sub>2</sub> to HCOOH using finite-temperature DFT metadynamics simulations. As a result, the barrier of the reaction was found to be 21.4 kcal mol<sup>-1</sup>. Jiang et al. [121] performed the screening of doped metals (i.e., Cr, Mn, Fe, Co, Ni, Cu, Zn, Rh, and Ir) on a porphyrin-based linker of MOF-525 and reached a similar conclusion. They found that the concerted pathway was kinetically favorable on

Ir@TCPP (tetrakis(4-carboxyphenyl)-porphyrin), where an approximately 18.0 kcal mol<sup>-1</sup> energy barrier is manifested on both hydrogen dissociation and CO<sub>2</sub> hydrogenation. Ye et al. [122] conducted a computational study of the concerted pathway on functionalized MOFs and revealed that MIL-140B-NBF<sub>2</sub> and MIL-140C-NBF<sub>2</sub> (Figure 5) outperformed UiO-66-P-BF<sub>2</sub> and UiO-67-NBF<sub>2</sub>, where high activity of P-BF<sub>2</sub> was identified in comparison with other functional groups of P series (i.e., P-B(NO<sub>2</sub>)<sub>2</sub>, P-B(CF<sub>2</sub>)<sub>2</sub>, P-B(CN)<sub>2</sub>, P-BBr<sub>2</sub>, P-BCl<sub>2</sub>, P-BH<sub>2</sub>, and P-B(CH3)<sub>2</sub>) screened on UiO-66 in a previous study [123,124]. In addition, a stepwise mechanism might be the predominant reaction on MOF. Mohmmad Faizan and Ravinder Pawaralanine demonstrated that the HCOO pathway is a more dominant route than the concerted pathway on boronic acid functionalized UiO-66 [125]. As demonstrated, the direct hydrogenation of the CO<sub>2</sub> and COOH pathways is seemingly not favorable on MOFs.

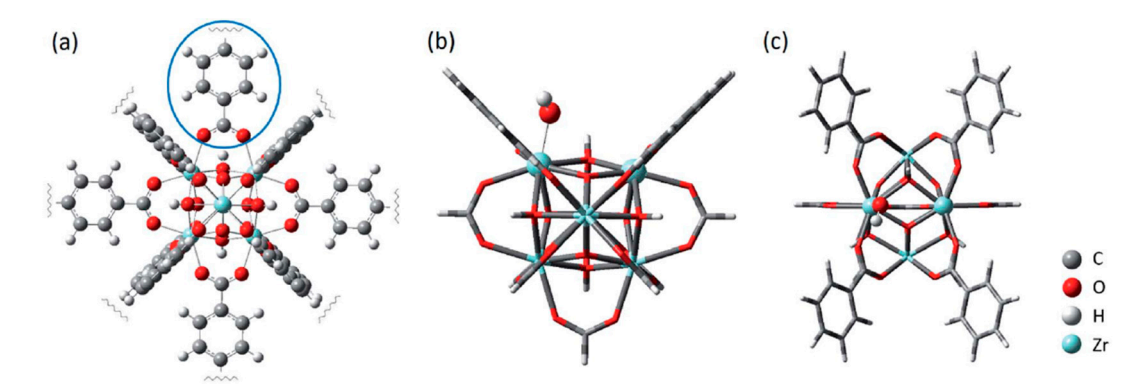


**Figure 4.** (a) A perfect UiO-66 node with twelve organic linkers. The linker in the blue circle is to be removed to create a frustrated Lewis pair (FLP). (b) Side and (c) top views of a small cluster. The open Zr site (Lewis acid), the adjacent hydroxide (Lewis base), and its bonded Zr atom are shown as balls. Adapted from ref. [117] with permission from The Royal Society of Chemistry, copyright 2020.

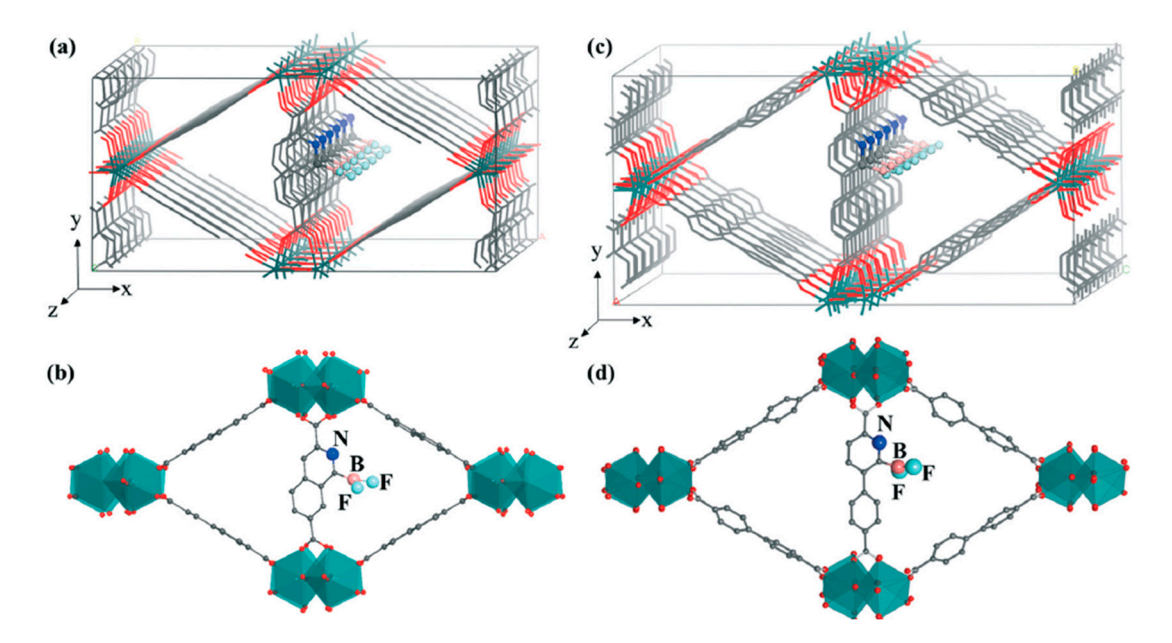


**Figure 5.** Structures of MIL-140B-NBF<sub>2</sub> and MIL-140C-NBF<sub>2</sub>. Parts (**a**,**c**) illustrate the framework showing six unit cells along the z direction. The framework atoms are represented by lines, and the LP functional moieties are represented by balls and sticks. Colors of the atoms are as follows: pink for B, grey for C, dark blue for N, red for O, light blue for F, and dark green for Zr. Parts (**b**,**d**) show unit cells of MIL-140B-NBF<sub>2</sub> and MIL-140C-NBF<sub>2</sub>, with Zr represented by a polyhedral and the other atoms represented by balls and sticks. [122] Adapted from ref. [122] with permission from The Royal Society of Chemistry, copyright 2018.

Catalysts 2025, 15, 978 14 of 20

On MNPs, stepwise mechanisms prevail in the absence of intrinsic FLP sites, with formate-type intermediates widely implicated [126–128]. Conversely, the presence of an organic ligand and metal ion on MCs can form FLPs, supporting both stepwise and concerted routes [109,129]. As the reactivity varies with chemical compositions of active sites [130–133], a mechanistic study should be carried out to screen the catalytic activities on MOFs, MCs, or MNPs, and the interfacial sites between them, to identify the dominant reaction route on MOF-confined catalysts. Nonetheless, no relevant work has hitherto been published, leaving the mechanism of thermal CO<sub>2</sub>-to-HCOOH conversion elusive on MC@MOF or MNP@MOF.

# 4. Conclusions and Perspective

We reviewed recent advances in thermal CO<sub>2</sub>-to-HCOOH conversion over metal complexes or MNPs stabilized by conventional heterogeneous supports or MOFs. MOFs are advantageous to high dispersion of the catalysts and the inhibition of metal aggregation by encapsulation, while conventional heterogeneous supports can hardly offer such merits. Given MOF-based confined catalysts for such thermal conversion are quite limited with respect to electrocatalysis and photocatalysis, we hereby offer the following perspectives in urging more extensive efforts to overcome the remaining challenges:

- (i) DFT calculations are recommended for an in-depth analysis of synergistic catalysis including the preferred reaction mechanism at the molecular level;
- (ii) Design MOFs with hierarchical porosity or controlled framework flexibility to overcome the limitations on the diffusion of reactants or products due to small pore structure;
- (iii) As ZIF and MIL series are usually operated at  $\leq$ 120 °C, far from the industrial level (i.e., 150 °C), hydrophobic functional groups and Zr/Ce nodes are suggested to reconfigure their SBUs to enhance hydrothermal stability.

**Author Contributions:** Z.Y.: writing—original draft, validation, formal analysis. W.X.: resources. H.C.: writing—review and editing. All authors have read and agreed to the published version of the manuscript.

Funding: This research received no external funding.

**Data Availability Statement:** The data in this review are summarized based on published works. For the acquisition of raw data, please refer to the cited literature in the References section.

Conflicts of Interest: The authors declare no conflicts of interest.

## References

- 1. Mac Dowell, N.; Fennell, P.S.; Shah, N.; Maitland, G.C. The Role of CO<sub>2</sub> Capture and Utilization in Mitigating Climate Change. *Nat. Clim. Chang.* **2017**, *7*, 243–249. [CrossRef]
- 2. Leitner, W. Carbon Dioxide as a Raw Material: The Synthesis of Formic Acid and Its Derivatives from CO<sub>2</sub>. *Angew. Chem. Int. Ed. Engl.* **1995**, *34*, 2207–2221. [CrossRef]
- 3. Inoue, Y.; Izumida, H.; Sasaki, Y.; Hashimoto, H. Catalytic Fixation of Carbon Dioxide to Formic Acid by Transition-Metal Complexes Under Mild Conditions. *Chem. Lett.* **1976**, *5*, 863–864. [CrossRef]
- 4. Wang, W.-H.; Bao, M.; Feng, X. *Transformation of Carbon Dioxide to Formic Acid and Methanol*, 1st ed.; SpringerBriefs in Green Chemistry for Sustainability; Springer: Singapore, 2018. [CrossRef]
- 5. Vieira, L.H.; Rasteiro, L.F.; Santana, C.S.; Catuzo, G.L.; Da Silva, A.H.M.; Assaf, J.M.; Assaf, E.M. Noble Metals in Recent Developments of Heterogeneous Catalysts for CO<sub>2</sub> Conversion Processes. *ChemCatChem* **2023**, *15*, e202300493. [CrossRef]
- 6. Gunasekar, G.H.; Park, K.; Jung, K.-D.; Yoon, S. Recent Developments in the Catalytic Hydrogenation of CO<sub>2</sub> to Formic Acid/Formate Using Heterogeneous Catalysts. *Inorg. Chem. Front.* **2016**, *3*, 882–895. [CrossRef]
- 7. Jessop, P.G.; Hsiao, Y.; Ikariya, T.; Noyori, R. Homogeneous Catalysis in Supercritical Fluids: Hydrogenation of Supercritical Carbon Dioxide to Formic Acid, Alkyl Formates, and Formamides. *J. Am. Chem. Soc.* **1996**, *118*, 344–355. [CrossRef]

8. Munshi, P.; Main, A.D.; Linehan, J.C.; Tai, C.-C.; Jessop, P.G. Hydrogenation of Carbon Dioxide Catalyzed by Ruthenium Trimethylphosphine Complexes: The Accelerating Effect of Certain Alcohols and Amines. *J. Am. Chem. Soc.* **2002**, *124*, 7963–7971. [CrossRef]

- 9. Elek, J.; Nádasdi, L.; Papp, G.; Laurenczy, G.; Joó, F. Homogeneous Hydrogenation of Carbon Dioxide and Bicarbonate in Aqueous Solution Catalyzed by Water-Soluble Ruthenium(II) Phosphine Complexes. *Appl. Catal. Gen.* **2003**, 255, 59–67. [CrossRef]
- 10. Himeda, Y. Conversion of CO<sub>2</sub> into Formate by Homogeneously Catalyzed Hydrogenation in Water: Tuning Catalytic Activity and Water Solubility through the Acid–Base Equilibrium of the Ligand. *Eur. J. Inorg. Chem.* **2007**, 2007, 3927–3941. [CrossRef]
- 11. Kipshagen, A.; Baums, J.C.; Hartmann, H.; Besmehn, A.; Hausoul, P.J.C.; Palkovits, R. Formic Acid as H<sub>2</sub> Storage System: Hydrogenation of CO<sub>2</sub> and Decomposition of Formic Acid by Solid Molecular Phosphine Catalysts. *Catal. Sci. Technol.* **2022**, 12, 5649–5656. [CrossRef]
- 12. Jessop, P.G.; Ikariya, T.; Noyori, R. Homogeneous Catalytic Hydrogenation of Supercritical Carbon Dioxide. *Nature* **1994**, *368*, 231–233. [CrossRef]
- Álvarez, A.; Bansode, A.; Urakawa, A.; Bavykina, A.V.; Wezendonk, T.A.; Makkee, M.; Gascon, J.; Kapteijn, F. Challenges in the Greener Production of Formates/Formic Acid, Methanol, and DME by Heterogeneously Catalyzed CO<sub>2</sub> Hydrogenation Processes. Chem. Rev. 2017, 117, 9804–9838. [CrossRef]
- 14. Centi, G.; Perathoner, S. Opportunities and Prospects in the Chemical Recycling of Carbon Dioxide to Fuels. *Catal. Today* **2009**, 148, 191–205. [CrossRef]
- 15. Wu, H.; Li, H.; Zhao, W.; Sudarsanam, P.; Yang, S. Protophilic Solvent-Impelled Quasi-Catalytic CO<sub>2</sub> Valorization to Formic Acid and N-Formamides. *Fuel* **2022**, *326*, 125074. [CrossRef]
- Franco, F.; Fernández, S.; Lloret-Fillol, J. Advances in the Electrochemical Catalytic Reduction of CO<sub>2</sub> with Metal Complexes. Curr. Opin. Electrochem. 2019, 15, 109–117. [CrossRef]
- 17. Ra, E.C.; Kim, K.Y.; Kim, E.H.; Lee, H.; An, K.; Lee, J.S. Recycling Carbon Dioxide through Catalytic Hydrogenation: Recent Key Developments and Perspectives. *ACS Catal.* **2020**, *10*, 11318–11345. [CrossRef]
- 18. Yan, N.; Philippot, K. Transformation of CO<sub>2</sub> by Using Nanoscale Metal Catalysts: Cases Studies on the Formation of Formic Acid and Dimethylether. *Curr. Opin. Chem. Eng.* **2018**, 20, 86–92. [CrossRef]
- 19. Li, H.; Peng, B.; Lv, S.; Zhou, Q.; Yan, Z.; Luan, X.; Liu, X.; Niu, C.; Liu, Y.; Hou, J. Immobilized Heterogeneous Catalysts for CO<sub>2</sub> Hydrogenation to Formic Acid: A Review. *Carbon Capture Sci. Technol.* **2024**, *13*, 100322. [CrossRef]
- Wang, Y.; Ma, J.-X.; Zhang, Y.; Xu, N.; Wang, X.-L. A Series of Cobalt-Based Coordination Polymer Crystalline Materials as Highly Sensitive Electrochemical Sensors for Detecting Trace Cr(VI), Fe(III) Ions, and Ascorbic Acid. Cryst. Growth Des. 2021, 21, 4390–4397. [CrossRef]
- 21. Ye, Z.; Xie, W.; Chen, H. Catalytic Hydrogenation of Carbon Dioxide to Methanol on MOF-Confined Metal Nanoparticles: A Review. *Catalysts* **2025**, *15*, 913. [CrossRef]
- 22. Yaghi, O.M.; Li, H. Hydrothermal Synthesis of a Metal-Organic Framework Containing Large Rectangular Channels. *J. Am. Chem. Soc.* 1995, 117, 10401–10402. [CrossRef]
- 23. Li, H.; Eddaoudi, M.; O'Keeffe, M.; Yaghi, O.M. Design and Synthesis of an Exceptionally Stable and Highly Porous Metal-Organic Framework. *Nature* **1999**, 402, 276–279. [CrossRef]
- 24. Freund, R.; Canossa, S.; Cohen, S.M.; Yan, W.; Deng, H.; Guillerm, V.; Eddaoudi, M.; Madden, D.G.; Fairen-Jimenez, D.; Lyu, H.; et al. 25 Years of Reticular Chemistry. *Angew. Chem. Int. Ed.* **2021**, *60*, 23946–23974. [CrossRef] [PubMed]
- Lu, X.; Song, C.; Qi, X.; Li, D.; Lin, L. Confinement Effects in Well-Defined Metal-Organic Frameworks (MOFs) for Selective CO<sub>2</sub>
  Hydrogenation: A Review. Int. J. Mol. Sci. 2023, 24, 4228. [CrossRef]
- 26. Liu, X.; Qian, B.; Zhang, D.; Yu, M.; Chang, Z.; Bu, X. Recent Progress in Host–Guest Metal–Organic Frameworks: Construction and Emergent Properties. *Coord. Chem. Rev.* **2023**, 476, 214921. [CrossRef]
- 27. Wang, W.; Wang, S.; Ma, X.; Gong, J. Recent Advances in Catalytic Hydrogenation of Carbon Dioxide. *Chem. Soc. Rev.* **2011**, 40, 3703. [CrossRef]
- 28. Bredig, G.; Carter, S.R. Katalytische Synthese der Ameisensäure unter Druck. *Berichte Dtsch. Chem. Ges.* **1914**, 47, 541–545. [CrossRef]
- 29. Sun, R.; Liao, Y.; Bai, S.-T.; Zheng, M.; Zhou, C.; Zhang, T.; Sels, B.F. Heterogeneous Catalysts for CO<sub>2</sub> Hydrogenation to Formic Acid/Formate: From Nanoscale to Single Atom. *Energy Environ. Sci.* **2021**, *14*, 1247–1285. [CrossRef]
- 30. Navarro-Jaén, S.; Virginie, M.; Bonin, J.; Robert, M.; Wojcieszak, R.; Khodakov, A.Y. Highlights and Challenges in the Selective Reduction of Carbon Dioxide to Methanol. *Nat. Rev. Chem.* **2021**, *5*, 564–579. [CrossRef]
- Lee, J.H.; Ryu, J.; Kim, J.Y.; Nam, S.-W.; Han, J.H.; Lim, T.-H.; Gautam, S.; Chae, K.H.; Yoon, C.W. Carbon Dioxide Mediated, Reversible Chemical Hydrogen Storage Using a Pd Nanocatalyst Supported on Mesoporous Graphitic Carbon Nitride. J. Mater. Chem. A 2014, 2, 9490. [CrossRef]
- 32. Wang, F.; Xu, J.; Shao, X.; Su, X.; Huang, Y.; Zhang, T. Palladium on Nitrogen-Doped Mesoporous Carbon: A Bifunctional Catalyst for Formate-Based, Carbon-Neutral Hydrogen Storage. *ChemSusChem* **2016**, *9*, 246–251. [CrossRef]

33. Park, H.; Lee, J.H.; Kim, E.H.; Kim, K.Y.; Choi, Y.H.; Youn, D.H.; Lee, J.S. A Highly Active and Stable Palladium Catalyst on a G-C<sub>3</sub>N<sub>4</sub> Support for Direct Formic Acid Synthesis under Neutral Conditions. *Chem. Commun.* **2016**, *52*, 14302–14305. [CrossRef]

- 34. Mondelli, C.; Puértolas, B.; Ackermann, M.; Chen, Z.; Pérez-Ramírez, J. Enhanced Base-Free Formic Acid Production from CO<sub>2</sub> on Pd/g-C<sub>3</sub>N<sub>4</sub> by Tuning of the Carrier Defects. *ChemSusChem* **2018**, *11*, 2859–2869. [CrossRef] [PubMed]
- 35. Zhang, Z.; Zhang, L.; Yao, S.; Song, X.; Huang, W.; Hülsey, M.J.; Yan, N. Support-Dependent Rate-Determining Step of CO<sub>2</sub> Hydrogenation to Formic Acid on Metal Oxide Supported Pd Catalysts. *J. Catal.* **2019**, *376*, 57–67. [CrossRef]
- 36. Min, B.K.; Santra, A.K.; Goodman, D.W. Understanding Silica-Supported Metal Catalysts: Pd/Silica as a Case Study. *Catal. Today* **2003**, *85*, 113–124. [CrossRef]
- 37. Zhang, Y.; Fei, J.; Yu, Y.; Zheng, X. Silica Immobilized Ruthenium Catalyst Used for Carbon Dioxide Hydrogenation to Formic Acid (I): The Effect of Functionalizing Group and Additive on the Catalyst Performance. *Catal. Commun.* **2004**, *5*, 643–646. [CrossRef]
- 38. Liu, N.; Du, R.J.; Li, W. Hydrogenation CO<sub>2</sub> to Formic Acid over Ru Supported on γ-Al<sub>2</sub>O<sub>3</sub> Nanorods. *Adv. Mater. Res.* **2013**, 821–822, 1330–1335. [CrossRef]
- 39. Hao, C.; Wang, S.; Li, M.; Kang, L.; Ma, X. Hydrogenation of CO<sub>2</sub> to Formic Acid on Supported Ruthenium Catalysts. *Catal. Today* **2011**, *160*, 184–190. [CrossRef]
- 40. Yu, Y.-M.; Fei, J.-H.; Zhang, Y.-P.; Zheng, X.-M. MCM-41 Bound Ruthenium Complex as Heterogeneous Catalyst for Hydrogenation I: Effect of Support, Ligand and Solvent on the Catalyst Performance. *Chin. J. Chem.* **2006**, 24, 840–844. [CrossRef]
- 41. Yu, Y.-M.; Zhang, Y.-P.; Fei, J.-H.; Zheng, X.-M. Silica Immobilized Ruthenium Catalyst for Formic Acid Synthesis from Supercritical Carbon Dioxide Hydrogenation II: Effect of Reaction Conditions on the Catalyst Performance. *Chin. J. Chem.* **2005**, 23, 977–982. [CrossRef]
- 42. Zhang, Z.; Xie, Y.; Li, W.; Hu, S.; Song, J.; Jiang, T.; Han, B. Hydrogenation of Carbon Dioxide Is Promoted by a Task-Specific Ionic Liquid. *Angew. Chem. Int. Ed.* **2008**, *47*, 1127–1129. [CrossRef] [PubMed]
- 43. Zhang, Z.; Hu, S.; Song, J.; Li, W.; Yang, G.; Han, B. Hydrogenation of CO<sub>2</sub> to Formic Acid Promoted by a Diamine-Functionalized Ionic Liquid. *ChemSusChem* **2009**, *2*, 234–238. [CrossRef]
- 44. Srivastava, V. Active Heterogeneous Ru Nanocatalysts for CO<sub>2</sub> Hydrogenation Reaction. *Catal. Lett.* **2016**, *146*, 2630–2640. [CrossRef]
- 45. Zhang, W.; Wang, S.; Zhao, Y.; Ma, X. Hydrogenation of scCO<sub>2</sub> to Formic Acid Catalyzed by Heterogeneous Ruthenium(III)/Al<sub>2</sub>O<sub>3</sub> Catalysts. *Chem. Lett.* **2016**, 45, 555–557. [CrossRef]
- 46. Zhang, W.; Wang, S.; Zhao, Y.; Ma, X. Hydrogenation of CO<sub>2</sub> to Formic Acid Catalyzed by Heterogeneous Ru-PPh3/Al<sub>2</sub>O<sub>3</sub> Catalysts. *Fuel Process. Technol.* **2018**, *178*, 98–103. [CrossRef]
- 47. Xu, Z.; McNamara, N.D.; Neumann, G.T.; Schneider, W.F.; Hicks, J.C. Catalytic Hydrogenation of CO<sub>2</sub> to Formic Acid with Silica-Tethered Iridium Catalysts. *ChemCatChem* **2013**, *5*, 1769–1771. [CrossRef]
- 48. McNamara, N.D.; Hicks, J.C. CO<sub>2</sub> Capture and Conversion with a Multifunctional Polyethyleneimine-Tethered Iminophosphine Iridium Catalyst/Adsorbent. *ChemSusChem* **2014**, 7, 1114–1124. [CrossRef]
- 49. Preti, D.; Resta, C.; Squarcialupi, S.; Fachinetti, G. Carbon Dioxide Hydrogenation to Formic Acid by Using a Heterogeneous Gold Catalyst. *Angew. Chem. Int. Ed.* **2011**, *50*, 12551–12554. [CrossRef] [PubMed]
- 50. Filonenko, G.A.; Vrijburg, W.L.; Hensen, E.J.M.; Pidko, E.A. On the Activity of Supported Au Catalysts in the Liquid Phase Hydrogenation of CO<sub>2</sub> to Formates. *J. Catal.* **2016**, *343*, 97–105. [CrossRef]
- 51. Qadir, M.I.; Weilhard, A.; Fernandes, J.A.; de Pedro, I.; Vieira, B.J.C.; Waerenborgh, J.C.; Dupont, J. Selective Carbon Dioxide Hydrogenation Driven by Ferromagnetic RuFe Nanoparticles in Ionic Liquids. *ACS Catal.* 2018, 8, 1621–1627. [CrossRef]
- 52. Mori, K.; Sano, T.; Kobayashi, H.; Yamashita, H. Surface Engineering of a Supported PdAg Catalyst for Hydrogenation of CO<sub>2</sub> to Formic Acid: Elucidating the Active Pd Atoms in Alloy Nanoparticles. *J. Am. Chem. Soc.* **2018**, *140*, 8902–8909. [CrossRef]
- 53. Mori, K.; Masuda, S.; Tanaka, H.; Yoshizawa, K.; Che, M.; Yamashita, H. Phenylamine-Functionalized Mesoporous Silica Supported PdAg Nanoparticles: A Dual Heterogeneous Catalyst for Formic Acid/CO<sub>2</sub>-Mediated Chemical Hydrogen Delivery/Storage. *Chem. Commun.* **2017**, *53*, 4677–4680. [CrossRef]
- 54. Masuda, S.; Mori, K.; Futamura, Y.; Yamashita, H. PdAg Nanoparticles Supported on Functionalized Mesoporous Carbon: Promotional Effect of Surface Amine Groups in Reversible Hydrogen Delivery/Storage Mediated by Formic Acid/CO<sub>2</sub>. *ACS Catal.* **2018**, *8*, 2277–2285. [CrossRef]
- 55. Masuda, S.; Mori, K.; Kuwahara, Y.; Yamashita, H. PdAg Nanoparticles Supported on Resorcinol-Formaldehyde Polymers Containing Amine Groups: The Promotional Effect of Phenylamine Moieties on CO<sub>2</sub> Transformation to Formic Acid. *J. Mater. Chem. A* **2019**, *7*, 16356–16363. [CrossRef]
- 56. Nguyen, L.T.M.; Park, H.; Banu, M.; Kim, J.Y.; Youn, D.H.; Magesh, G.; Kim, W.Y.; Lee, J.S. Catalytic CO<sub>2</sub> Hydrogenation to Formic Acid over Carbon Nanotube-Graphene Supported PdNi Alloy Catalysts. *RSC Adv.* **2015**, *5*, 105560–105566. [CrossRef]
- 57. Motokura, K.; Kashiwame, D.; Miyaji, A.; Baba, T. Copper-Catalyzed Formic Acid Synthesis from CO<sub>2</sub> with Hydrosilanes and H<sub>2</sub>O. Org. Lett. **2012**, *14*, 2642–2645. [CrossRef]

Catalysts 2025, 15, 978 17 of 20

58. Cauwenbergh, R.; Goyal, V.; Maiti, R.; Natte, K.; Das, S. Challenges and Recent Advancements in the Transformation of CO<sub>2</sub> into Carboxylic Acids: Straightforward Assembly with Homogeneous 3d Metals. *Chem. Soc. Rev.* **2022**, *51*, 9371–9423. [CrossRef]

- 59. Chiang, C.-L.; Lin, K.-S.; Chuang, H.-W. Direct Synthesis of Formic Acid via CO<sub>2</sub> Hydrogenation over Cu/ZnO/Al<sub>2</sub>O<sub>3</sub> Catalyst. *J. Clean. Prod.* **2018**, 172, 1957–1977. [CrossRef]
- 60. Chiang, C.-L.; Lin, K.-S.; Chuang, H.-W.; Wu, C.-M. Conversion of Hydrogen/Carbon Dioxide into Formic Acid and Methanol over Cu/CuCr<sub>2</sub>O<sub>4</sub> Catalyst. *Int. J. Hydrogen Energy* **2017**, *42*, 23647–23663. [CrossRef]
- 61. Liu, X.; Zhong, H.; Wang, C.; He, D.; Jin, F. CO<sub>2</sub> Reduction into Formic Acid under Hydrothermal Conditions: A Mini Review. *Energy Sci. Eng.* **2022**, *10*, 1601–1613. [CrossRef]
- 62. Lyu, L.; Zeng, X.; Yun, J.; Wei, F.; Jin, F. No Catalyst Addition and Highly Efficient Dissociation of H<sub>2</sub>O for the Reduction of CO<sub>2</sub> to Formic Acid with Mn. *Environ. Sci. Technol.* **2014**, *48*, 6003–6009. [CrossRef] [PubMed]
- 63. Yao, G.; Zeng, X.; Jin, Y.; Zhong, H.; Duo, J.; Jin, F. Hydrogen Production by Water Splitting with Al and In-Situ Reduction of CO<sub>2</sub> into Formic Acid. *Int. J. Hydrogen Energy* **2015**, *40*, 14284–14289. [CrossRef]
- 64. Duo, J.; Jin, F.; Wang, Y.; Zhong, H.; Lyu, L.; Yao, G.; Huo, Z. NaHCO<sub>3</sub> -Enhanced Hydrogen Production from Water with Fe and in Situ Highly Efficient and Autocatalytic NaHCO<sub>3</sub> Reduction into Formic Acid. *Chem. Commun.* **2016**, *52*, 3316–3319. [CrossRef] [PubMed]
- 65. Jiang, H.; Alezi, D.; Eddaoudi, M. A Reticular Chemistry Guide for the Design of Periodic Solids. *Nat. Rev. Mater.* **2021**, *6*, 466–487. [CrossRef]
- 66. Eddaoudi, M.; Moler, D.B.; Li, H.; Chen, B.; Reineke, T.M.; O'Keeffe, M.; Yaghi, O.M. Modular Chemistry: Secondary Building Units as a Basis for the Design of Highly Porous and Robust Metal—Organic Carboxylate Frameworks. *Acc. Chem. Res.* **2001**, *34*, 319–330. [CrossRef]
- 67. Chen, Z.; Kirlikovali, K.O.; Li, P.; Farha, O.K. Reticular Chemistry for Highly Porous Metal–Organic Frameworks: The Chemistry and Applications. *Acc. Chem. Res.* **2022**, *55*, 579–591. [CrossRef]
- 68. Schukraft, G.E.M.; Ayala, S.; Dick, B.L.; Cohen, S.M. Isoreticular Expansion of polyMOFs Achieves High Surface Area Materials. *Chem. Commun.* **2017**, *53*, 10684–10687. [CrossRef]
- 69. Bigdeli, F.; Fetzer, M.N.A.; Nis, B.; Morsali, A.; Janiak, C. Coordination Modulation: A Way to Improve the Properties of Metal–Organic Frameworks. *J. Mater. Chem. A* **2023**, *11*, 22105–22131. [CrossRef]
- 70. Ding, M.; Flaig, R.W.; Jiang, H.-L.; Yaghi, O.M. Carbon Capture and Conversion Using Metal–Organic Frameworks and MOF-Based Materials. *Chem. Soc. Rev.* **2019**, *48*, 2783–2828. [CrossRef]
- 71. Liu, K.-G.; Sharifzadeh, Z.; Rouhani, F.; Ghorbanloo, M.; Morsali, A. Metal-Organic Framework Composites as Green/Sustainable Catalysts. *Coord. Chem. Rev.* **2021**, 436, 213827. [CrossRef]
- 72. Li, S.; Huo, F. Metal–Organic Framework Composites: From Fundamentals to Applications. *Nanoscale* **2015**, 7, 7482–7501. [CrossRef]
- 73. Luo, W.; Zhang, Z.; Zhu, G.; Zhang, X.; Huang, G.; Zhou, T.; Lu, X. Precise Pore Regulation Strategies for Constructing High-Performance Metal–Organic Framework (MOF) Membranes for Gas Capture: Frontier Advances. *J. Environ. Chem. Eng.* 2025, 13, 118229. [CrossRef]
- 74. Wen, Y.; Zhang, P.; Sharma, V.K.; Ma, X.; Zhou, H.-C. Metal-Organic Frameworks for Environmental Applications. *Cell Rep. Phys. Sci.* **2021**, *2*, 100348. [CrossRef]
- 75. Zhang, J.; An, B.; Li, Z.; Cao, Y.; Dai, Y.; Wang, W.; Zeng, L.; Lin, W.; Wang, C. Neighboring Zn–Zr Sites in a Metal–Organic Framework for CO<sub>2</sub> Hydrogenation. *J. Am. Chem. Soc.* **2021**, *143*, 8829–8837. [CrossRef]
- 76. Sabo, M.; Henschel, A.; Fröde, H.; Klemm, E.; Kaskel, S. Solution Infiltration of Palladium into MOF-5: Synthesis, Physisorption and Catalytic Properties. *J. Mater. Chem.* **2007**, *17*, 3827. [CrossRef]
- 77. Maksimchuk, N.; Timofeeva, M.; Melgunov, M.; Shmakov, A.; Chesalov, Y.; Dybtsev, D.; Fedin, V.; Kholdeeva, O. Heterogeneous Selective Oxidation Catalysts Based on Coordination Polymer MIL-101 and Transition Metal-Substituted Polyoxometalates. *J. Catal.* 2008, 257, 315–323. [CrossRef]
- 78. Mandal, T.; Kumar, R.; Kumar, S.; Choudhury, J. Single-Site Heterogenized Molecular Catalysts towards CO<sub>2</sub> Hydrogenation to Formates, Formamides and Methanol. *ChemCatChem* **2024**, *16*, e202400272. [CrossRef]
- 79. Shao, S.; Cui, C.; Tang, Z.; Li, G. Recent Advances in Metal-Organic Frameworks for Catalytic CO<sub>2</sub> Hydrogenation to Diverse Products. *Nano Res.* **2022**, *15*, 10110–10133. [CrossRef]
- 80. Shi, Y.; Hou, S.; Qiu, X.; Zhao, B. MOFs-Based Catalysts Supported Chemical Conversion of CO<sub>2</sub>. *Top. Curr. Chem.* **2020**, *378*, 11. [CrossRef]
- 81. Liu, K.-G.; Bigdeli, F.; Panjehpour, A.; Larimi, A.; Morsali, A.; Dhakshinamoorthy, A.; Garcia, H. Metal Organic Framework Composites for Reduction of CO<sub>2</sub>. *Coord. Chem. Rev.* **2023**, 493, 215257. [CrossRef]
- 82. Liu, M.; Peng, Y.; Chen, W.; Cao, S.; Chen, S.; Lu Meng, F.; Jin, Y.; Hou, C.-C.; Zou, R.; Xu, Q. Metal-Organic Frameworks for Carbon-Neutral Catalysis: State of the Art, Challenges, and Opportunities. *Coord. Chem. Rev.* **2024**, *506*, 215726. [CrossRef]

83. Chuanchuan, D.; Yuling, L.; Hao, S.; Shuaishuai, L.; Qiyuan, S.; Xinzeng, L. Evolutionary Trends and Photothermal Catalytic Reduction Performance of Carbon Dioxide by MOF-Derived MnOx. *Fuel* **2025**, *384*, 133949. [CrossRef]

- 84. Wu, C.; Irshad, F.; Luo, M.; Zhao, Y.; Ma, X.; Wang, S. Ruthenium Complexes Immobilized on an Azolium Based Metal Organic Framework for Highly Efficient Conversion of CO<sub>2</sub> into Formic Acid. *ChemCatChem* **2019**, *11*, 1256–1263. [CrossRef]
- 85. Xu, L.; Cui, T.; Zhu, J.; Wang, X.; Ji, M. PdAg Alloy Nanoparticles Immobilized on Functionalized MIL-101-NH<sub>2</sub>: Effect of Organic Amines on Hydrogenation of Carbon Dioxide into Formic Acid. *New J. Chem.* **2021**, 45, 6293–6300. [CrossRef]
- 86. Tshuma, P.; Makhubela, B.C.E.; Bingwa, N.; Mehlana, G. Palladium(II) Immobilized on Metal–Organic Frameworks for Catalytic Conversion of Carbon Dioxide to Formate. *Inorg. Chem.* **2020**, *59*, 6717–6728. [CrossRef]
- 87. Gumbo, M.; Makhubela, B.C.E.; Amombo Noa, F.M.; Öhrström, L.; Al-Maythalony, B.; Mehlana, G. Hydrogenation of Carbon Dioxide to Formate by Noble Metal Catalysts Supported on a Chemically Stable Lanthanum Rod-Metal-Organic Framework. *Inorg. Chem.* 2023, 62, 9077–9088. [CrossRef]
- 88. Nilwanna, K.; Sittiwong, J.; Boekfa, B.; Treesukol, P.; Boonya-udtayan, S.; Probst, M.; Maihom, T.; Limtrakul, J. Aluminum-based Metal-organic Framework Support Metal(II)-Hydride as Catalyst for the Hydrogenation of Carbon Dioxide to Formic Acid: A Computational Study. *Mol. Catal.* 2023, 541, 113116. [CrossRef]
- 89. Dhakshinamoorthy, A.; Navalón, S.; Primo, A.; García, H. Selective Gas-Phase Hydrogenation of CO<sub>2</sub> to Methanol Catalysed by Metal-Organic Frameworks. *Angew. Chem. Int. Ed.* **2024**, *63*, e202311241. [CrossRef] [PubMed]
- 90. Kaishyop, J.; Gahtori, J.; Dalakoti, S.; Gazi, M.J.; Khan, T.S.; Bordoloi, A. Sorption Enhanced CO<sub>2</sub> Hydrogenation to Formic Acid over CuZn-MOF Derived Catalysts. *J. Mater. Chem. A* **2024**, *12*, 8457–8473. [CrossRef]
- 91. Chen, L.; Chen, H.; Luque, R.; Li, Y. Metal—organic Framework Encapsulated Pd Nanoparticles: Towards Advanced Heterogeneous Catalysts. *Chem. Sci.* **2014**, *5*, 3708–3714. [CrossRef]
- 92. Ge, X.; Wong, R.; Anisa, A.; Ma, S. Recent Development of Metal-Organic Framework Nanocomposites for Biomedical Applications. *Biomaterials* **2022**, *281*, 121322. [CrossRef]
- 93. Chen, L.; Luque, R.; Li, Y. Controllable Design of Tunable Nanostructures inside Metal–Organic Frameworks. *Chem. Soc. Rev.* **2017**, *46*, 4614–4630. [CrossRef]
- 94. Li, Y.-M.; Hu, J.; Zhu, M. Confining Atomically Precise Nanoclusters in Metal–Organic Frameworks for Advanced Catalysis. *Coord. Chem. Rev.* **2023**, 495, 215364. [CrossRef]
- 95. Zheng, F.; Zhang, W.; Guo, Q.; Yu, B.; Wang, D.; Chen, W. Metal Clusters Confined in Porous Nanostructures: Synthesis, Properties and Applications in Energy Catalysis. *Coord. Chem. Rev.* **2024**, *502*, 215603. [CrossRef]
- 96. Bavykina, A.; Kolobov, N.; Khan, I.S.; Bau, J.A.; Ramirez, A.; Gascon, J. Metal–Organic Frameworks in Heterogeneous Catalysis: Recent Progress, New Trends, and Future Perspectives. *Chem. Rev.* **2020**, *120*, 8468–8535. [CrossRef]
- 97. Chen, L.; Xu, Q. Metal-Organic Framework Composites for Catalysis. Matter 2019, 1, 57–89. [CrossRef]
- 98. Wang, Y.; Ling, L.; Zhang, W.; Guo, J.; Ding, K.; Duan, W.; Liu, B. "Ship-in-Bottle" Strategy to Encapsulate Shape-Controllable Metal Nanocrystals into Metal–Organic Frameworks: Internal Space Matters. *Chem. Mater.* **2019**, *31*, 9546–9553. [CrossRef]
- 99. Fernández-Conde, C.; Zheng, Y.; Mon, M.; Ribera, A.; Leyva-Pérez, A.; Martí-Gastaldo, C. Time-Resolved Control of Nanoparticle Integration in Titanium-Organic Frameworks for Enhanced Catalytic Performance. *Chem. Sci.* **2024**, *15*, 2351–2358. [CrossRef]
- 100. Kim, J.S.; Chang, H.; Kang, S.; Cha, S.; Cho, H.; Kwak, S.J.; Park, N.; Kim, Y.; Kang, D.; Song, C.K.; et al. Critical Roles of Metal-Ligand Complexes in the Controlled Synthesis of Various Metal Nanoclusters. *Nat. Commun.* 2023, 14, 3201. [CrossRef] [PubMed]
- 101. Li, X.; Zeng, Z.; Zeng, G.; Wang, D.; Xiao, R.; Wang, Y.; Zhou, C.; Yi, H.; Ye, S.; Yang, Y. A "Bottle-around-Ship" like Method Synthesized Yolk-Shell Ag<sub>3</sub>PO<sub>4</sub>@MIL-53(Fe) Z-Scheme Photocatalysts for Enhanced Tetracycline Removal. *J. Colloid Interface Sci.* 2020, 561, 501–511. [CrossRef]
- 102. Hermes, S.; Schröter, M.-K.; Schmid, R.; Khodeir, L.; Muhler, M.; Tissler, A.; Fischer, R.W.; Fischer, R.A. Metal@MOF: Loading of Highly Porous Coordination Polymers Host Lattices by Metal Organic Chemical Vapor Deposition. *Angew. Chem. Int. Ed.* 2005, 44, 6237–6241. [CrossRef]
- 103. Paparo, A.; Okuda, J. Carbon Dioxide Complexes: Bonding Modes and Synthetic Methods. *Coord. Chem. Rev.* **2017**, 334, 136–149. [CrossRef]
- 104. Wang, S.; Hou, S.; Wu, C.; Zhao, Y.; Ma, X. RuCl<sub>3</sub> Anchored onto Post-Synthetic Modification MIL-101(Cr)-NH<sub>2</sub> as Heterogeneous Catalyst for Hydrogenation of CO<sub>2</sub> to Formic Acid. *Chin. Chem. Lett.* **2019**, *30*, 398–402. [CrossRef]
- 105. Hu, X.; Luo, M.; ur Rehman, M.; Sun, J.; Yaseen, H.A.S.M.; Irshad, F.; Zhao, Y.; Wang, S.; Ma, X. Mechanistic Insight into the Electron-Donation Effect of Modified ZIF-8 on Ru for CO<sub>2</sub> Hydrogenation to Formic Acid. *J. CO2 Util.* **2022**, *60*, 101992. [CrossRef]
- 106. Ohnishi, Y.; Nakao, Y.; Sato, H.; Sakaki, S. Ruthenium(II)-Catalyzed Hydrogenation of Carbon Dioxide to Formic Acid. Theoretical Study of Significant Acceleration by Water Molecules. *Organometallics* **2006**, 25, 3352–3363. [CrossRef]
- 107. Wen, M.; Mori, K.; Futamura, Y.; Kuwahara, Y.; Navlani-García, M.; An, T.; Yamashita, H. PdAg Nanoparticles within Core-Shell Structured Zeolitic Imidazolate Framework as a Dual Catalyst for Formic Acid-Based Hydrogen Storage/Production. Sci. Rep. 2019, 9, 15675. [CrossRef]

108. Wu, C.; Luo, M.; Zhao, Y.; Wang, S.; Ma, X.; Zavabeti, A.; Xiao, P.; Li, G.K. CO<sub>2</sub> Hydrogenation Using MOFs Encapsulated PdAg Nano-Catalysts for Formate Production. *Chem. Eng. J.* **2023**, 475, 146411. [CrossRef]

- 109. An, B.; Zeng, L.; Jia, M.; Li, Z.; Lin, Z.; Song, Y.; Zhou, Y.; Cheng, J.; Wang, C.; Lin, W. Molecular Iridium Complexes in Metal–Organic Frameworks Catalyze CO<sub>2</sub> Hydrogenation via Concerted Proton and Hydride Transfer. *J. Am. Chem. Soc.* **2017**, 139, 17747–17750. [CrossRef] [PubMed]
- 110. Li, Z.; Rayder, T.M.; Luo, L.; Byers, J.A.; Tsung, C.-K. Aperture-Opening Encapsulation of a Transition Metal Catalyst in a Metal-Organic Framework for CO<sub>2</sub> Hydrogenation. *J. Am. Chem. Soc.* **2018**, *140*, 8082–8085. [CrossRef]
- 111. Howarth, A.J.; Liu, Y.; Li, P.; Li, Z.; Wang, T.C.; Hupp, J.T.; Farha, O.K. Chemical, Thermal and Mechanical Stabilities of Metal–Organic Frameworks. *Nat. Rev. Mater.* **2016**, *1*, 15018. [CrossRef]
- 112. Park, J.; Kim, H.S.; Lee, W.B.; Park, M.-J. Trends and Outlook of Computational Chemistry and Microkinetic Modeling for Catalytic Synthesis of Methanol and DME. *Catalysts* **2020**, *10*, 655. [CrossRef]
- 113. Odoh, S.O.; Cramer, C.J.; Truhlar, D.G.; Gagliardi, L. Quantum-Chemical Characterization of the Properties and Reactivities of Metal–Organic Frameworks. *Chem. Rev.* 2015, 115, 6051–6111. [CrossRef]
- 114. Jiao, L.; Jiang, H.-L. Metal-Organic Frameworks for Catalysis: Fundamentals and Future Prospects. *Chin. J. Catal.* **2023**, 45, 1–5. [CrossRef]
- 115. Coufourier, S.; Gaillard, S.; Clet, G.; Serre, C.; Daturi, M.; Renaud, J.-L. A MOF-Assisted Phosphine Free Bifunctional Iron Complex for the Hydrogenation of Carbon Dioxide, Sodium Bicarbonate and Carbonate to Formate. *Chem. Commun.* **2019**, *55*, 4977–4980. [CrossRef]
- 116. Rohde, R.C.; Carsch, K.M.; Dods, M.N.; Jiang, H.Z.H.; McIsaac, A.R.; Klein, R.A.; Kwon, H.; Karstens, S.L.; Wang, Y.; Huang, A.J.; et al. High-Temperature Carbon Dioxide Capture in a Porous Material with Terminal Zinc Hydride Sites. *Science* 2024, 386, 814–819. [CrossRef]
- 117. Yang, K.; Jiang, J. Computational Design of a Metal-Based Frustrated Lewis Pair on Defective UiO-66 for CO<sub>2</sub> Hydrogenation to Methanol. *J. Mater. Chem. A* **2020**, *8*, 22802–22815. [CrossRef]
- 118. Ali Akbar Razavi, S.; Morsali, A. Linker Functionalized Metal-Organic Frameworks. *Coord. Chem. Rev.* **2019**, 399, 213023. [CrossRef]
- 119. Maihom, T.; Wannakao, S.; Boekfa, B.; Limtrakul, J. Production of Formic Acid via Hydrogenation of CO<sub>2</sub> over a Copper-Alkoxide-Functionalized MOF: A Mechanistic Study. *J. Phys. Chem. C* **2013**, *117*, 17650–17658. [CrossRef]
- 120. Heshmat, M. Alternative Pathway of CO<sub>2</sub> Hydrogenation by Lewis-Pair-Functionalized UiO-66 MOF Revealed by Metadynamics Simulations. *J. Phys. Chem. C* **2020**, 124, 10951–10960. [CrossRef]
- 121. Krishnan, R.; Yang, K.; Hashem, K.; Jiang, J. Metallated Porphyrinic Metal—organic Frameworks for CO<sub>2</sub> Conversion to HCOOH: A Computational Screening and Mechanistic Study. *Mol. Catal.* **2022**, *527*, 112407. [CrossRef]
- 122. Ye, J.; Li, L.; Johnson, J.K. The Effect of Topology in Lewis Pair Functionalized Metal Organic Frameworks on CO<sub>2</sub> Adsorption and Hydrogenation. *Catal. Sci. Technol.* **2018**, *8*, 4609–4617. [CrossRef]
- 123. Ye, J.; Johnson, J.K. Screening Lewis Pair Moieties for Catalytic Hydrogenation of CO<sub>2</sub> in Functionalized UiO-66. *ACS Catal.* **2015**, 5, 6219–6229. [CrossRef]
- 124. Ye, J.; Johnson, J.K. Design of Lewis Pair-Functionalized Metal Organic Frameworks for CO<sub>2</sub> Hydrogenation. *ACS Catal.* **2015**, *5*, 2921–2928. [CrossRef]
- 125. Faizan, M.; Pawar, R. Alanine Boronic Acid Functionalized UiO-66 MOF as a Nanoreactor for the Conversion of CO<sub>2</sub> into Formic Acid. *J. Comput. Chem.* **2023**, *44*, 1624–1633. [CrossRef] [PubMed]
- 126. Peng, G.; Sibener, S.J.; Schatz, G.C.; Mavrikakis, M. CO<sub>2</sub> Hydrogenation to Formic Acid on Ni(110). *Surf. Sci.* **2012**, *606*, 1050–1055. [CrossRef]
- 127. Yan, G.; Gao, Z.; Zhao, M.; Yang, W.; Ding, X. CO<sub>2</sub> Hydrogenation to Formic Acid over Platinum Cluster Doped Defective Graphene: A DFT Study. *Appl. Surf. Sci.* **2020**, *517*, 146200. [CrossRef]
- 128. Ye, Z.; Chen, H. Mechanistic Study of CO<sub>2</sub> Hydrogenation to HCOOH on Copper Nanocluster. *Chem. Phys. Lett.* **2025**, 878, 142378. [CrossRef]
- 129. Naimatullah; Cui, Y.; Yuan, Q.; Cheng, L. Theoretical Calculation of Single-Atom Supported BN Catalyzing CO<sub>2</sub> Hydrogenation to Formic Acid: A First Principles Study. *Chem. Phys.* **2025**, *597*, 112781. [CrossRef]
- 130. Noh, G.; Lam, E.; Bregante, D.T.; Meyet, J.; Šot, P.; Flaherty, D.W.; Copéret, C. Lewis Acid Strength of Interfacial Metal Sites Drives CH<sub>3</sub> OH Selectivity and Formation Rates on Cu-Based CO<sub>2</sub> Hydrogenation Catalysts. *Angew. Chem. Int. Ed.* **2021**, *60*, 9650–9659. [CrossRef]
- 131. Wang, J.; Song, Y.; Li, J.; Liu, F.; Wang, J.; Lv, J.; Wang, S.; Li, M.; Bao, X.; Ma, X. Modulation of Al<sub>2</sub>O<sub>3</sub> and ZrO<sub>2</sub> Composite in Cu/ZnO-Based Catalysts with Enhanced Performance for CO<sub>2</sub> Hydrogenation to Methanol. *Appl. Catal. Gen.* **2024**, *674*, 119618. [CrossRef]

Catalysts 2025, 15, 978 20 of 20

132. Zhang, H.; Yang, J.; Wang, S.; Zhao, N.; Xiao, F.; Wang, Y. Effect of Ni Content on Cu–Mn/ZrO<sub>2</sub> Catalysts for Methanol Synthesis from CO<sub>2</sub> Hydrogenation. *Catal. Sci. Technol.* **2024**, *14*, 2153–2165. [CrossRef]

133. Pimbaotham, P.; Injongkol, Y.; Jungsuttiwong, S.; Yodsin, N. Advancing CO<sub>2</sub> Hydrogenation to Formic Acid: DFT Insights into Frustrated Lewis Pair—Functionalized UiO—67 Catalysts. *J. Catal.* **2024**, *436*, 115571. [CrossRef]

**Disclaimer/Publisher's Note:** The statements, opinions and data contained in all publications are solely those of the individual author(s) and contributor(s) and not of MDPI and/or the editor(s). MDPI and/or the editor(s) disclaim responsibility for any injury to people or property resulting from any ideas, methods, instructions or products referred to in the content.